# Designing Against Size Effect on Shear Strength of Reinforced Concrete Beams Without Stirrups

By Zdeněk P. Bažant[1] and Qiang Yu[2]

**Abstract:** The shear failure of reinforced concrete beams is a very complex fracture phenomenon for which a purely mathematical modeling approach is not possible at present. However, detailed modeling of the fracture mechanism is not necessary for establishing the general form of the size effect. The mere knowledge of the fact that the failure is caused by cohesive (quasibrittle) fracture propagation and that the maximum load is attained only after large fracture growth (and not at fracture initiation) is shown to suffice for determining the general approximate mathematical form of the size effect law, while the numerical coefficients of this law need to be identified from experimental data. Simple dimensional analysis yields the asymptotic properties of size effect, which are characterized by (1) a constant beam shear strength $v_c$ (i.e., absence of size effect) for sufficiently small beam depths, and (2) the LEFM size effect $v_c \sim d^{-1/2}$ for very large beam depths $d$. Together with the known small- and large-size second-order asymptotic properties of the cohesive (or fictitious) crack model, this suffices to unambiguously support a size effect formula of the general approximate form $v_c = v_0(1+d/d_0)^{-1/2}$ (where $v_0, d_0$ are constants), which was proposed in 1984 for shear failure of beams on the basis of less general and less fundamental arguments. Calibration by least-square regression of the existing experimental database (consisting of 398 data) leads to several empirical expressions for $v_0$ and $d_0$ with different compromises between accuracy and simplicity.

## Introduction

Although a provision for size effect in shear failure of reinforced concrete beams was incorporated into some design codes more than a dozen years ago, a compelling experimental evidence obtained with properly scaled large-size beams made of normal concrete has become available only during the last few years. The case has now become clear: The design formula must include the size effect. The problem is how to best interpret the test results and how to best describe the size effect mathematically in a sufficiently simple and practical manner without violating certain restrictions that have crystallized from theoretical researches during the last two decades. To clarify this timely question, is the objective of this article.

The size effect is measured in terms of the nominal strength, generally defined as $\sigma_N = P/bd$ where $P$ is the maximum (or ultimate) load (or load parameter), $b$ is the structure width and $d$ is the characteristic dimension (or size) of the structure. The size effect is characterized by comparing $\sigma_N$ for geometrically similar structures of different sizes $d$. According to the classical allowable stress design, as well as the theory of limit states (or plastic limit analysis) which underlies the current design codes for reinforced concrete structures, the nominal strength $\sigma_N$ is independent of the structure size. We say that in this case there is no size effect. It has been generally proven that the size effect is absent from all structural analysis methods in which the material failure at a point of the structure is decided by the stress and strain tensors at that point. If the material failure criterion involves energy, a size effect inevitably arises. This

[1]McCormick School Professor and W.P. Murphy Professor of Civil Engineering and Materials Science, Northwestern University, Tech-CEE, 2145 Sheridan Rd., Evanston, Illinois 60208; z-bazant@northwestern.edu.

[2]Graduate Research Assistant, Northwestern University.

is the case of fracture mechanics, provided that either the crack or the fracture process zone (microcracking zone) at failure (or both) is not negligible compared to structure dimensions.

A size effect is exhibited by all the theories of failure which involve some material characteristic length, $l_0$. This is always the case when the failure criterion involves some quantity of the dimensions of energy. An example is the cohesive crack model, as well as the crack band model, which is almost equivalent. The cohesive (or fictitious) crack model, pioneered for concrete by Hillerborg, is now regarded as the best among the simple approximate models for concrete fracture.

## Method of Interpretation of Existing Experimental Database

Why can't a size effect formula be determined purely empirically? We need to address this question to place the problem in proper perspective. Many formulas in concrete design codes can of course be developed purely empirically because it is possible to obtain adequate test data for the entire range of practical interest, and to sample that range statistically uniformly, without bias. An example is the ratio of tensile and compressive strengths, or the effect of reinforcement ratio in various code specifications. Unfortunately, the size effect is not a problem of that kind.

Fig. 1 shows the histogram of the number of test data in ACI-445 database as a function of beam depth $d$. The size effect is of practical concern mainly for beam depths ranging from 1 m to 10 m. Unfortunately, 86% of all the available test data pertain to beam depths less than 0.5 m, and 99% to depths less than 1.1 m. The coefficient of variation $\omega$ of the deviations of a size effect formula from the points of the database will therefore be totally dominated by small depths for which the size effect is unimportant. Thus it can easily happen that some formula that gives the smallest $\omega$ for such data could be completely wrong for very large sizes while another formula that might give a higher $\omega$ could be much more realistic for large sizes. This is not the way to justify a formula for the ACI code. For an unbiased purely empirical validation of a formula, the test data would have to be distributed uniformly over the entire range of interest. In view of the costs of large scale tests, we cannot even hope to acquire such a database.

Therefore, we must extrapolate. Such extrapolation, visualized by Fig. 1, cannot be accomplished empirically. In keeping with the motto of ACI president's inaugural message [42], "ars sine scientia nihil est", a sound theoretical support is required. The theory, in turn should be verified by properly scaled size effect tests on one and the same concrete, and especially by reduced-scale model tests in which the dimensionless sizes (characterized in a shape-independent manner by their brittleness numbers $\beta$ [12, 24], defined later), can reach the highest possible values.

A size effect formula for shear strength, motivated by fracture mechanics, was proposed in 1984 [15]. Since that time a number of other formulas have appeared; see Fig. 2 which includes:

- the size effect law based on fracture mechanics and energy release arguments [5, 12, 14, 24];
- an extended form of that law for fractures in which the cohesive stresses are never reduced to zero but exhibit a finite residual strength [6];
- the CEB-FIP formula, introduced empirically [34];
- the formula of Japan Concrete Institute [43], motivated by Weibull theory, in which the failure is assumed to occur right at the initiation of a macroscopic crack and the size effect

is assumed to be caused by randomness of local material strength;

- a formula resulting from an enhancement of the modified compression field theory (MCFT) based on a supposed effect of crack spacing [1, 31, 33, 65]; and
- a power law corresponding to linear elastic fracture mechanics (LEFM) and supplemented with an upper bound (small-size cut-off).

For comparison, all the data points of the existing ACI-445 database are also shown in Fig. 2. What is striking in this figure is that the very different curves of the aforementioned formulas look almost equally good, or equally bad. The reason is that the size range covered by the data is not broad enough and the scatter is enormous. The size range cannot be significantly extended without very large financial outlays. The enormous scatter is caused by mixing in one database test data for different concretes, different shear spans, different reinforcement ratios, etc. These influences cannot be eliminated because they are highly random and poorly understood. The problem is compounded by the fact that most of the data sets included in the database involve only a single beam size (depth) or a negligible size range (as their original purpose was to clarify influences other than the size effect).

Some efforts are presently being made to choose among various formulas by comparing the coefficients of variation of the errors of each formula calculated for the existing ACI-445 database. But such efforts are futile. The coefficients of variation of the deviations of the formula from the data points are almost the same for all the formulas, good or bad. The arbitrariness of such a comparison then inevitably leads a committee to a political choice.

The most serious obstacle to extracting size effect information from the ACI-445 database is the fact that the vast majority (more than 97%) of its 398 data points come from tests motivated by different objectives (such as the effect of concrete type, reinforcement, shear span, etc.), in which the beam depth was not varied at all. To document the problem, see Fig. 3, which shows some such test data (marked by an oval) in comparison with the size effect law [5] and (at bottom right) with the data points from two tests series of the broadest available size range. These data contaminate the database by unnecessary scatter due to influences that cannot be eliminated because they are poorly understood. Such contamination greatly widens the scatter band of the database and masks the size effect trends of the individual data series with a significant size range. When this database is fitted with a power law (a straight line in the figure), the exponent (slope of the straight line) will depend on size distribution of the data; see Fig. 5 which illustrates how the shifting of a hypothetical data cloud to smaller or larger sizes can lead any power law exponent between 0 and $-1/2$. Obviously, such statistical inferences are not objective; they depend on the frequency of test data in various size intervals, which is a subjective choice of the experimenters influenced by the funds available.

So is the existing ACI-445 database useless? Not at all. But it should be used *only* for calibrating the size effect formula after the *basic form* of that formula has already been selected, and nothing else. The selection of the best form of the formula must be based on a sound theory. The theory should of course be experimentally validated. This can be done only by comparisons with individual test series with proper scaling and a broad enough size range, made on one and the same concrete. The theory must be such that it could also capture similar size effects in other types of failure with the same physical source, occurring in concrete as well as other quasibrittle materials. Because of the typical high random scatter in beam shear tests, the size range should be at least 1:8. Geometrical similarity of the beams of various sizes should be maintained as closely as possible, so as to prevent pollution of the data set by uncertain influences other than those of the size. Currently there exist only about 11 data series (from 8 investigator teams [1, 3, 14, 31, 40, 44, 50, 63]) satisfying these criteria at least to some extent

(a few more have a significant size range but grossly violate geometrical similarity). Only two of them, namely the 1991 Northwestern tests [14] and the recent Toronto tests [1, 31], satisfy these criteria quite closely. Of these two, the Northwestern ones [14] are reduced-scale model tests, which have the advantage that they achieve (thanks to the reduced scale) the largest dimensionless size so far (as measured by the brittleness number [24]).

Recently it was attempted to deflect the foregoing criticism by considering only the aforementioned test series in which the beam depth was significantly varied. However, the combined group of such test series was evaluated jointly, without paying attention to the trends of the individual test series. This is again misleading. To illustrate it, consider Fig. 4 showing bi-logarithmic plots of $\log v_c$ versus $\log d$ (on the left) for two sets of four hypothetical data series with the same range of beam depth $d$ (in log-scale), generated so as to match *perfectly* the curves of the theoretical size effect law $v_c = v_0(1 + d/d_0)^{-1/2}$ (discussed later), in which $v_0$ and $d_0$ are empirical parameters depending on the type of concrete. The set on top is obtained by a frugal investigator, who has modest funding and must therefore test smaller (less expensive) beams, and the set at the bottom is obtained by a wealthy investigator, who has greater funding and can thus afford to test larger beams. Each investigator conducts the size effect tests for four different concretes each of which is the same for both investigators (and all the other influencing parameters, including the steel ratio $\rho$ and shear span $a/d$, are also the same for both). The curve of the size effect law for each concrete is different, characterized by different values $v_{01}, v_{02}, d_{01}, d_{02}$ of the size effect law parameters $v_0$ and $d_0$. Assuming that both of these investigators do not know the theoretical size effect law and regard these perfect data as one combined database, they see only the data pictures on the right of Fig. 4. Because of the high scatter of the combined database on the right, each investigator, looking at his combined database, can at best infer a straight line trend in the bi-logarithmic plot, which corresponds to a power-law size effect. By statistical regression, the frugal investigator thus finds the mean size effect $v_c \propto d^{-1/4}$ (which happens to coincide with the JSCE code specification [43]), while the wealthy investigator finds the mean size effect $v_c \propto d^{-1/3}$ (which happens to coincide with a recent recommendation by one code-proposing subcommittee). Thus, because they have not checked the trends of the individual data series, both investigators are led to erroneous conclusions. Their conclusions depend on subjective factors, such as the choice of beam sizes which, in turn, depends on the funding of their sponsors. Making the tests for variously shifted size ranges, these investigators could have obtained as optimum *any exponent* between 0 and $-1/2$; see Fig. 5. Obviously, knowledge of a sound theory and of the trends of the individual test series is needed to obtain the correct conclusion.

## Variables in the Problem of Failure and Size Effect

Problems of quasibrittle fracture in the normal range of interest are very difficult to solve. However, the asymptotic properties are simple. For very small structure sizes, the asymptotic solution can be obtained by plastic limit analysis, and for very large sizes, by linear elastic fracture mechanics (LEFM—a theory in which the fracture process zone is a point and the structure, which may be inelastic, unloads during fracture propagation elastically). These asymptotic situations are often outside the size range of practical interest (being approached closely, for example, only for 'concrete' beams 1 mm deep and 100 m deep, respectively). It is nevertheless very helpful to know these asymptotic situations because a good approximate solution for the intermediate practical size range can be obtained by some sort of 'interpolation' between these asymptotic cases, called asymptotic matching.

Although the detailed mechanism of shear failure of reinforced concrete beams is complicated, it clearly consists of some complex form of cohesive softening fracture. The material softening due to distributed fracturing may also be taking place but because it must localize into narrow bands, it may be approximated as cohesive softening fracture. This fact alone suffices to establish the basic asymptotic properties of size effect.

The problem of shear capacity of the cross section involves the following variables:

- The shear strength $v_c$ which we want to predict, defined as $v_c = V/b_w d$ ($v_c$ plays here the role of nominal strength of structure, normally denoted as $\sigma_N$); $V$ = shear force, which is assumed to be distributed uniformly, $d$ depth from the top face of beam to the centroid of longitudinal reinforcement, and $b_w$ width of the web, which equals the total beam width $b$ if the cross section is rectangular.

- The characteristic size of the structure, chosen as $d$.

- Parameters $G_f$ and $\sigma_0$ of the cohesive crack model, which automatically exhibits size effect [12, 26]. This model was developed by Barenblatt [4], Leonov and Panasyuk [51], Rice [61], Palmer and Rice [56] and others (Knauss, Smith, Wnuk and Kfouri and Rice[47, 48, 64, 67, 46]), and was pioneered for concrete by Hillerborg et al. [39] under the name fictitious crack model [24, 58]. Fracture energy $G_f$ represents the area under the initial tangent of the softening curve of cohesive stress versus crack-face separation (Fig. 6). The shape of the softening curve is assumed to be fixed, which means that all the other parameters of the softening curve, such as the total fracture energy $G_F$, representing the area under the entire curve, are related to $\sigma_0$ and $G_f$.

- Geometry parameters $\rho = A_s/b_w d$, $L/d, L_1/d, L_2/d, ...$, which represent the reinforcement ratio ($A_s$ = cross section area of steel) and the ratios to $d$ of all dimensions $L, L_1, L_2, ...$ defining the span $L$, the beam length, the cover thickness, and the distances defining the locations of loading points. The beam width $b_w$ need not be included since its effect on $v_c$ is known to be negligible. Some of the parameters $L_i$ characterize the crack shape and crack tip location at maximum load.

Normally the cohesive crack model is considered to describe the tensile fracture, in which case $\sigma_0 = f'_t$ = tensile strength of concrete. However, the shear failure of beam is doubtless triggered by shear-compression fracture of concrete in the region above the tip of the main crack and delamination fracture of concrete cover (as a result of dowel action) and bond fracture (propagation of a crack along the steel concrete interface, with subsidiary cracks emanating from bar deformations) may also play some role.[3] In the case of crack band or cohesive crack models for compression fracture, the strength limit is the compressive strength $\sigma_0 = f'_c$, and in the case of bond fracture it is the bond strength. For our general dimensional analysis, we do not need to distinguish among these diverse strength limits (and that is why the strength is generally denoted as $\sigma_0$). The fracture energy together with $\sigma_0$ imply a material characteristic length,

$$l_0 \;=\; E G_f \;/\; {\sigma_0}^2 \tag{1}$$

[3]Note that compression shear-fracture (or compression crushing), which is an essential criterion for brittle failure in the strut-and-tie model, exhibits a pronounced size effect and is also described by the crack-band model (in the form of triaxial softening damage) or by the cohesive crack model (adapted for compression). Likewise, the cover delamination and propagation of bond fracture also require cohesive crack model.

introduced by Irwin's [41] for metals and by Hillerborg for concrete; $l_0$ characterizes the length of the fracture process zone at the tip of a crack or crack band.

The solution represents a functional relation which may generally be written as

$$\Phi(v_c, \sigma_0, EG_f, d, \rho, L, L_1, L_2, ..., L_{m-1}) = 0 \tag{2}$$

Here we multiply $G_f$ with Young's elastic modulus $E$ because it is known that maximum loads in fracture mechanics do not depend separately on $E$ and $G_f$ but only on their product representing the fracture toughness, given by Irwin's relation $K_c = \sqrt{EG_f}$. In (2), we have a total of $N_t = 5 + m$ parameters.[4]

## Small- and Large-Size Asymptotes Dictated by Dimensional Analysis

The number of unknowns may be reduced by introducing dimensionless parameters. According to the Buckingham's Π-theorem[5] [28], the number, $n$, of independent dimensionless parameters is equal to the total number, $n_t$, of all parameters minus the number of independent physical dimensions. Combining this theorem with the known physical meaning of $l_0$, we can determine the asymptotic behaviors.

First, consider that $l_0 \ll d$. Since $l_0$ is known to characterize the size of the fracture process zone, it follows that this zone becomes infinitely smaller than $d$. This means that, in relation to the beam depth, all of fracture is happening at only one point, which propagates. Consequently, the material strength $\sigma_0$ can have no effect and can be removed from the list of parameters in (2). Function $\Phi$ of $5 + m$ parameters then becomes a function, $\hat{\Phi}$, of $4 + m$ parameters, i.e.

$$\hat{\Phi}(v_c, EG_f, d, \rho, L, L_1, L_2, ..., L_{m-1}) = 0 \tag{4}$$

There are only two independent physical dimensions, Pa and m (in SI units), because the dimensions of all the other parameters in (2) can be obtained as products and ratios of Pa and m (for instance, the physical dimension of $EG_f$ is, in SI units, Pa×J/m$^2$ or N$^2$/m$^3$). Therefore, according to the Π-theorem, the problem of failure can be recast as a functional relation among $2 + m$ dimensionless parameters, which may be chosen as follows:

$$\hat{\phi}({v_c}^2 d/EG_f, \rho, L/d, L_1/d, L_2/d, ..., L_{m-1}/d) = 0 \tag{5}$$

If the structures of different sizes $d$ are geometrically similar (which includes the condition that the main cracks in specimens of different sizes must be similar), then $\rho, L/d, L_1/d, L_2/d, ...$ are all constant, and so the first parameter in the foregoing equation must also be constant, i.e,, ${v_c}^2 d/EG_f =$ constant. It follows that

$$\text{for } \; d \gg l_0 : \qquad v_c \;=\; C_0 \sqrt{\frac{EG_f}{d}} \;=\; \frac{\text{constant}}{\sqrt{d}} \tag{6}$$

[4]Based on Eqs. 9–11 for the fracturing truss model [9], an example of function $\Phi$ is

$$\Phi(v_c, ...) = k_e {v_c}^2 (1 + a^2/d^2) - EG_f/(1 + d/\kappa_e l_0) = 0 \tag{3}$$

where $k_e$ and $\kappa_e$ are empirical functions of $f'_c$ and $\rho$. However, although this model yields a realistic form of size effect, it turned out to be insufficient to capture realistically the effects of other influencing parameters, including $a/d$, $\rho$, $f'_c$ and $d_a$. This is why we must justify the size effect by general dimensional analysis which is valid regardless of the details of the model and influences other than the size.

[5]This theorem would be more properly called Riabouchinsky-Buckingham's theorem since the idea was introduced earlier by Riabouchinski [60].

where $C_0$ is a constant depending on the geometry parameters.

Note that the foregoing argument requires that the fracture length at the moment of failure must not be negligible. When the failure occurs right at fracture initiation from a smooth surface (as in the modulus of rupture test of flexural strength of unreinforced beams), then the last equation does not apply because the energy release rate of an infinitely short crack is zero.

Eq. (6) is a power scaling law that is characteristic of linear elastic fracture mechanics (LEFM), observed in the case that the cracks at maximum load are large and geometrically similar, or that the structures contain geometrically similar notches.[6] In a plot of $\log v_c$ versus $\log d$, this asymptotic scaling is represented by a straight line of slope $-1/2$.

Second, consider that $l_0 \gg d$. In this case the fracture process zone occupies the entire cross section, and so there can be no fracture propagation. So, the failure load must be independent of $K_c$ or $EG_f$. According to the Π-theorem, the problem again reduces to a functional relation among $2 + m$ dimensionless parameters, which may be chosen as follows:

$$\tilde{\phi}(v_c/\sigma_0, \rho, L/d, L_1/d, L_2/d, ..., L_{m-1}/d) = 0 \tag{7}$$

Noting again that, for geometrically similar structures, $\rho, L/d, L_1/d, L_2/d, ...$ are constant, we conclude that the first parameter in the foregoing equation must also be constant, i.e,, $v_c/\sigma_0 =$ constant, and so

$$\text{for } \; d \ll l_0 : \qquad v_c \; = \; C_1 \; \sigma_0 \; = \; \text{constant} \tag{8}$$

where $C_1 =$ constant. So, in this asymptotic case the size effect is absent. This is characteristic of plastic limit analysis as well as any theory in which the material failure condition is expressed in terms of stresses and strains.

The foregoing asymptotic scaling laws represent all that can be deduced from dimensional analysis alone. To learn more, one must take into account some results deduced from the differential equations and boundary conditions governing the mechanics of failure.

## Second-Order Asymptotic Properties

It has been generally proven [12] that the first two terms of the small-size and large-size asymptotic expansions of size effect based on the cohesive (or fictitious) crack model must have the following form:

$$\text{for } d \to 0: \qquad \frac{v_c}{C_0 \sigma_0} = 1 - \frac{d}{d_1} - ... \tag{9}$$

$$\text{for } d \to \infty: \qquad \frac{v_c}{C_1 \sigma_0} = \frac{1}{\sqrt{d}} \left( 1 - \frac{d_0}{2d} + ... \right) \tag{10}$$

([12], Eqs. 9.125, 9.126); $d_0$, $d_1$, $C_0$ and $C_1$ are constants with respect to the size effect (i.e., they depend on structure geometry but not on size $d$). These asymptotic properties hold true under the condition that the softening stress-separation curve of the cohesive crack model begins its descent with a finite slope, which is known to be true for concrete.

The asymptotic properties in (8) and (6) apply to all types of failure due to cohesive fracture or localization of distributed damage, provided that either there are large notches (which is

[6] The power law of exponent $-1/3$, i.e. $v_c \propto D^{-1/3}$, which has recently been proposed on the basis of the ACI-445 database contaminated by variation of highly scattered variables other than $d$, would be justified by dimensional analysis only if the fracture energy had the irrational dimension of $\text{J/m}^{7/3}$ instead of $\text{J/m}^2$ (where J = Nm = Joule).

not our case) or large geometrically similar fractures develop in a stable manner prior to the maximum load. The fact that the fracture patterns in small and large beams are approximately similar is documented by many laboratory experiments as well as finite element simulations. If, for example, the depths of fracture at maximum load in small and large beams were 20% and 80% of cross section depth, respectively, or if the fractures in small beams were almost vertical and in large beams almost horizontal, then this assumption would not apply. But from experience this is not the case.

The foregoing opposite asymptotic properties have been analytically derived by transformations of the differential equations and boundary conditions of continuum mechanics. The large-size asymptotic properties have further been derived by asymptotic expansion of (a) equivalent LEFM, or (b) the J-integral, or (c) the smeared-tip method [12].

Knowing these properties, one can extend dimensional analysis to obtain a simple expression for the transition between the asymptotes, which we do next.

## Size Effect Transition Between the Asymptotes

The fact that there are only two independent physical dimensions, Pa and m (in SI units) means, that according to the Π-theorem, the number of independent dimensionless variables is $n = 3 + m$. Although various sets of dimensionless parameters can be introduced, agreement with the asymptotic conditions (8) and (6) can be achieved by the following choice of $3 + m$ dimensionless parameters:

$$\Pi_1 = \frac{{v_c}^2 d}{E G_f} = \frac{{v_c}^2}{{\sigma_0}^2}\frac{d}{l_0}, \quad \Pi_2 = \frac{{v_c}^2}{{\sigma_0}^2}, \quad \Pi_3 = \rho, \quad \Pi_4 = \frac{L}{d}, \quad ...\Pi_n = \frac{L_{m-1}}{d} \tag{11}$$

The equation governing the nominal strength of structure may then be written as

$$F(\ \Pi_1,\ \Pi_2, ...\Pi_n\ ) = 0 \tag{12}$$

The fact that this choice of parameters agrees with the first-order asymptotic properties in (8) and (6) may be checked as follows.

For $d \to 0$, Eq. (12) takes the form:

$$F(\ 0,\ \Pi_2, ...\ ) = 0 \tag{13}$$

Noting that all the parameters other than $\Pi_2$ are constant (and that function $F$ must be, for physical reasons, uniquely invertible), we see that $\Pi_2$ must be constant, too, i.e. $v_c/\sigma_0 =$ constant, which agrees with (8).

For $d \to \infty$, Eq. (12) takes the form:

$$F(\ \Pi_1,\ 0, ...\ ) = 0 \tag{14}$$

Again, noting that all the parameters other than $\Pi_1$ are constant, we may conclude that the first parameter, $\Pi_1 = (v_c/\sigma_0)^2 d/l_0$, must be constant, too. This agrees with (6).

Let us now try to obtain a simple transitional size effect law which also agrees with the second-order terms in (9) and (10). To this end, we may expand function $F(\Pi_1, \Pi_2, ...)$ into a Taylor series about some chosen state $(D^*, v^*)$ in the middle of the ranges of $\Pi_1$ and $\Pi_2$;

$$\Delta F = F^* + F_1 \Delta\Pi_1 + F_2 \Delta\Pi_2 + \ ... \ = \ 0 \tag{15}$$

where
$$\Delta\Pi_1 = ({v_c}^2 D - {v^*}^2 D^*)/{\sigma_0}^2 l_0, \qquad \Delta\Pi_2 = ({v_c}^2 - {v^*}^2)/{\sigma_0}^2 \tag{16}$$

Here $F_1 = \partial F/\partial \Pi_1$ and $F_2 = \partial F/\partial \Pi_2$ are derivatives evaluated at that chosen state. Keeping only the linear terms as shown[7] and solving this equation for $\sigma_N$, we obtain an expression of the following general form [5, 23]:

$$\boxed{v_c = \frac{v_0}{\sqrt{1 + d/d_0}}} \tag{17}$$

in which $v_0$ and $d_0$ are constants which are expressed in terms of $D^*, v^*, F^*, F_1, F_2, \sigma_0$ and $l_0$ (and depend, in an unknown way, on structure shape). This formula, representing the first-order asymptotic matching, describes a smooth transition between the aforementioned two asymptotes (Fig. 2); $d_0$ is the transitional structure size, separating sizes $d > d_0$ for which the failure is predominantly brittle from sizes $d < d_0$ for which the failure is predominantly ductile (for this reason, the ratio $\beta = d/d_0$ is called the brittleness number [24, 6]). The use of this size effect law for shear failure of beams was proposed in 1984 [15], although on the basis of a much more restrictive and simplified mathematical argument.

The acceptability of the size effect law in (17) depends on satisfying both the first and second-order asymptotic terms in (9) and (10). This is readily checked by denoting $\beta = d/d_0$ and $\xi = d_0/d$, and realizing that

$$\text{for } \beta \ll 1: \qquad (1+\beta)^{-1/2} \approx 1 - \beta/2 \tag{18}$$

$$\text{for } \xi \ll 1: \qquad (1+1/\xi)^{-1/2} = \xi^{1/2}(1+\xi)^{-1/2} \approx \sqrt{\xi}(1-\xi/2) \tag{19}$$

Note that the foregoing derivation of size effect law has not relied on continuum mechanics. Even if a specimen or structure is not large enough compared to material inhomogeneities (aggregate size), the foregoing derivation remains valid because, even for random discrete media, the shear force $V$, material strength $\sigma_0$ and fracture energy $G_f$ can be defined statistically.

## The Question of Uniqueness of Size Effect Law

Let us now discuss the question of uniqueness of results. From the point of view of dimensional analysis, it would be perfectly legitimate to choose other dimensionless variables. If we chose $\Pi_1 = (v_c/\sigma_0)\sqrt{d/l_0}$ and $\Pi_2 = v_c/l_0$ and proceeded in the same manner as before, we would get the result $v_c = v_0/(1 + \sqrt{d/d_0})$, which is different from (17). Although this expression has the same asymptotes as the size effect law in (17), it disagrees with the second-order asymptotic terms in both (9) and (10), and so it must be ruled out.

As another example, one could take $\Pi_1 = {v_c}^p/{\sigma_0}^p(d/l_0)^q$ and $\Pi_2 = {v_c}^r/{\sigma_0}^r$ with any constants $p, q, r$. But then it would be found that, unless $p = r = 2$ and $q = 1$, the result would disagree with even the first-order asymptotic properties in asymptotic terms in (9) and (10).

On the other hand, nothing would, for example, prevent us from taking $\Pi_1 = {v_c}^2/{\sigma_0}^2(d/l_0)(1+ d^2/{l_0}^2)$. In that case, the asymptotic terms in (9) and (10) would be satisfied up to the second order, but the size effect expression would become considerably more complex.

[7] Including higher-order terms of Taylor series expansion, one could obtain higher-order asymptotic matching approximations capable of greater accuracy over a very broad size range (which have previously been obtained in other ways [10, 12]). But their greater complexity is, for concrete beams, unwarranted, in view of high scatter of test results.

So. Eq. (17) appears to be the only *simple* size effect formula satisfying the required first- and second-order asymptotic properties in (9) and (10).

There are also physical arguments that lead to dimensionless variables $\Pi_1$ and $\Pi_2$ as chosen. These variables characterize failure in terms of energy. $\Pi_1$ represents (except for a geometry-dependent factor) the ratio of the energy release rate of a crack to $G_f$, which is what decides the propagation of a crack when the structure is much larger than the fracture process zone. $\Pi_2$ represents (except for a geometry-dependent factor) the ratio of the strain energy density to its value at the strength limit of the material, which is what decides failure when the structure is smaller than a fully developed fracture process zone.

For data fitting, the size effect law in (17) or (22) has the advantage that it can be algebraically converted to a linear regression plot:

$$Y = Ad + C \tag{20}$$

$$\text{where} \qquad Y = \frac{1}{(v_c - v_r)^2}, \quad v_0 = \frac{1}{\sqrt{C}}, \quad d_0 = \frac{C}{A} \tag{21}$$

(Fig. 7 right). The regression is a convenient way to identify $v_0$ and $d_0$ from size effect test data.

For less complex problems in which the fracture path is simple and known, the size effect law in (17) has also been derived by several other methods, e.g., by asymptotic expansion of equivalent LEFM, asymptotic expansion of J-integral, and asymptotic expansion of smeared-tip method [12]. The first of these methods further yields expressions for the size effect parameters in terms of the energy release function of fracture mechanics. Such expressions, however, cannot be obtained for the beam shear problem because the LEFM crack pattern corresponding to infinite size extrapolation is unknown.

The size effect law in (17) has been verified numerically for many problems by finite element simulations based on nonlocal damage model, cohesive crack models, and lattice or particle models of microstructure. Experimental verifications now include many types of failure of reinforced concrete structures, as well as rocks, toughened ceramics, fiber composites, brittle foams, snow slabs and sea ice (the last up to a record size of 80m × 80m × 1.8m). In view of all this evidence, accumulated over the past two decades, it would be extremely surprising if the size effect law in (17) did not provide a good approximation for the shear failure of reinforced concrete beams.[8]

## Comparison with Individual Size Effect Data

The form of the size effect formula must be checked by comparison with data sets that are not significantly contaminated by variation of parameters other than size $d$. Ideally, the beams

[8]So far we have tacitly assumed that cohesive fracture reduces the stress all the way to zero. In compression fracture, though, if the softening zone is sufficiently confined so as to develop large frictional stresses, it is possible [12] that cohesive fracture terminates with some finite residual compressive stress. In that case, the foregoing dimensional analysis remains valid if $v_c$ is replaced by $v_c - v_r$, and the resulting formula, called the extended size effect law, has the form:

$$v_c = \frac{v_0}{\sqrt{1 + d/d_0}} + v_r \tag{22}$$

However, in the case of shear failure of normal reinforced concrete beams there is no way to develop a triaxial confinement strong enough to generate high frictional resistance in the ligament above the tip of the diagonal shear crack. Therefore (even though a finite value of $v_r$ makes it possible to obtain a slightly lower coefficient of variation for the entire ACI-445 database), formula (22) is not developed in detail.

tested must be geometrically scaled, cover a large size range, and use one and the same concrete (identically cured and tested under the same environmental conditions). Only two data sets came close to this ideal situation:

- Reduced-scale tests in 1991 at Northwestern University [14], in which beams having depths from 0.021 m to 0.33 m, maximum aggregate size 4.8 mm and reduced-scale bars with standard ASTM deformations (bought from PCA, Skokie) were tested (with 3 identical beams for each size); and
- recent normal-scale tests at the University of Toronto [1, 31], with beam depths from 0.11 m to 1.89 m and maximum aggregate size 10 mm (only one specimen of each size was tested, with an interval of up to two years elapsing between subsequent tests).

Eq. (17) leads to a very good agreement with both data series, as can be seen from the optimum fits of these data. This is documented by Fig. 7, and validates the correctness of the form of the formula. Three kinds of comparisons are shown: those with the Northwestern data alone (on top), those with the Toronto data alone (in the middle), and those with both data combined (at the bottom). In the last case, the optimum fit has been obtained under the constraint that the minimum relative values of $v_c/v_{c0}$ would be the same in both cases.

The optimum fits in Fig. 7 (on both the left and right) have been obtained by least-square fitting in the logarithmic scale using the Levenberg-Marquardt nonlinear optimization algorithm. The optimum parameters of the size effect formula (17) are given in the figures, along with the coefficient of variation which is defined later. All the fits are shown both in the plots of $\log(v_c/v_0)$ versus $\log(d/d_0)$ (on the left), and in linear regression plots of $(v_0/v_c)^2$ versus $d/d_0$ (on the right). The top two rows show the individual fits of each data set, and the last row shows a combined fit of both data sets obtained by constrained optimization already described.

Although linear regression in transformed variables has not been used to get the optimum fit, the linear regression plots are also shown in Fig. 7, on the right, along with their coefficients of variation. The results of nonlinear optimization and linear regression are close but not identical. The nonlinear optimization is slightly preferable because it implies a better weighting of the data [24].

What is particularly noteworthy is that the test series at both Northwestern University and University of Toronto verify very well the asymptotic behavior of fracture mechanics required by the foregoing asymptotic arguments coupled with dimensional analysis (Eq. 6). This confirms that the asymptotic slope of size effect in a doubly logarithmic plot must be $-1/2$.

In addition, it must be emphasized that the well-known Japanese tests [40, 63] do not at all contradict this asymptotic slope, even though they were previously interpreted by a power law of exponent $-1/4$; see Fig. 8. By implication, the comparisons with all the relevant test data thus confirm that the correct explanation of the size effect lies in fracture mechanics. This further verifies that the correctness of choosing $G_f$ and $\sigma_0$ as the governing material parameters in dimensional analysis.

The fact that the test data are much closer to the LEFM asymptote of slope $-1/2$ than to the horizontal asymptote means that the shear failure of beams is highly brittle. This further implies that the fracture energy is a much more important material parameter than the material strength, and that, if finite element programs are used, they must be based on fracture mechanics (as another consequence, the importance of introducing without delay a standardized fracture test of concrete [26] is highlighted).

Additional 7 data sets with a much narrower but non-negligible size range exist [44, 50, 3]. They are shown in Fig. 9. Unfortunately, geometrical similarity of scaling was significantly vio-

lated in these tests, due to variation of other influencing parameters such as $a/d$ and $\rho$. Because of uncertain influence of such parameters, these differences are simply neglected in making the comparisons in the figure, but the inevitable result is an increased scatter. Nevertheless, the size effect trend of these data is still described reasonably well, and the asymptotic slope $-1/2$ is not contradicted.

## Expressions for Size Effect Law Parameters

The question now is how to predict the values of $v_0$ and $d_0$. Expressions for these constants were set up in 1984 [15] on the basis of certain simplifications based on the beam theory and the idea of arch action, which however were superseded by later research. Further study [9] led to an energetic fracturing generalization of the truss model (also called the strut-and-tie model), which was based on a simplified estimation of the energy release rate from either the potential energy or the complementary energy (under the hypothesis that the failure at maximum load is triggered by propagation of a compression damage band of a fixed width across the compression strut). Such analysis led rigorously to the size effect law (17), which provided additional valuable support for the general form of this law, and it also gave an intuitive explanation as to why a size effect must arise. Recent comparisons with numerous test data from the databases compiled at Northwestern University and in ACI Committee 445 have nevertheless revealed that the detailed mechanism of failure assumed in [9] for the fracturing truss model was too simplified for capturing the dependence of coefficients $v_0$ and $d_0$ on parameters other than size $d$, particularly the dependence on $a/d$ and $\rho$. It transpired that the axis of the compression strut cannot be assumed to pass through the points of application of the load and the reaction. A much steeper compression strut (sketched in Fig. 10, top left) would have to be considered, but the proper slope to consider is unclear.

Therefore, we need to set up semi-empirical expressions for $v_0$ and $d_0$, which need to be calibrated by an experimental database. The following general expressions have been considered in optimization exercises:

$$d_0 = c_0 f_c'^{r_1} \rho^{r_2} (a/d)^{r_3} {d_a}^{r_4} \tag{23}$$

$$v_0 = k_0 f_c'^{r_5} \rho^{r_6} (a/d)^{r_7}, \tag{24}$$

where $k_0, c_0, r_1, ...r_7$ are empirical constants; $a/d$ = shear span (Fig. 6), $\rho$ = steel ratio, $f_c'$ = compressive strength of concrete, and $d_a$ = maximum aggregate size. Why don't we use the $\Pi$-theorem to reduce these expressions to a dimensionless form?—because we do not know all the influencing parameters. And why do we assume products of powers in these expressions?—in order to preclude the possibility of negative values and to have at the same time a linear form in terms of the logarithms.

## Calibration by Data Fitting

Coefficients $c_0, k_0, r_1, r_2, ...$ of the formulas for $v_0$ and $d_0$ have been calibrated by least-square optimum fitting of the ACI-445 database, consisting of 398 data points (see Fig. 2 and the dimensionless plots in Figs. 11–13). This database includes only the tests made under three-point loading, and therefore excludes the Japanese tests for record-size beams [40, 63] made under distributed loading.[9] Although most tests in the database had rectangular cross sections,

[9]The reduced-scale three-point-loaded tests at Northwestern University [14] were also excluded by ACI-445 from its database, based on three questionable arguments: (1) that the aggregate was supposedly too small

24 old ones had a T-cross section (these tests correspond to the upper left points in the diagrams in Figs. 11–13, deviating from the general trend and causing an increase in the standard error of regression).

The data fitting is a nonlinear statistical regression problem, and the choice of approach calls for some discussion. Let us denote by $\hat{v}_i$ ($i = 1, 2, ...n, n = 398$) the measured data points, and by $v_i$ the corresponding values of $v_c$ calculated from the formula. It appears that the best approach (Appendix II) is not to minimize sum of squared errors (or residuals) $\sum_i (v_i - \hat{v}_i)^2$ because the variance of data (or the scatter band width) decreases with the increasing size (i.e., the data are heteroskedastic). To minimize statistical bias, one should transform the statistical variable $v_c$ so as to make the variance approximately uniform (i.e., make the data approximately homoskedastic, independent of $d$). This may be achieved by least-square fitting in the logarithmic scale of $v_c$, i.e., by minimizing the square of the standard error of regression, $s_L$, the unbiased definition of which is

$$s_L{}^2 \;=\; \frac{1}{n-p} \sum_{i=1}^{n} \left( \ln \frac{v_i}{\hat{v}_i} \right)^2 \tag{25}$$

where $p$ is the number of free parameters in data fitting; in our problem, $p$ is at least 4 (parameters $c_0, k_0, r_1, r_2$) and better 5 (with $r_3$) (the reason why $p > 0$ is that $p$ data points can be fitted perfectly). Because $(\mathrm{d} \ln v_c)^2 = (\mathrm{d}v_c)^2 / {v_c}^2$, the scale transformation from linear to logarithmic has a similar effect as applying weights proportional to $1/{v_c}^2$ (except for the fact that the implied error distribution is gaussian in the scale of $\ln v_c$ rather than $v_c$). The minimization was accomplished by a standard library subroutine for the Levenberg-Marquardt nonlinear optimization algorithm, which reduces the problem to a sequence of linear regressions. Since $s_L$, defined in the scale of natural (not decadic) logarithm of $v_c$, is dimensionless, it may at the same time be regarded as the coefficient of variation. The reverse transformation to the linear scale of $v_c$ gives the following coefficient of variation of regression, characterizing the ratio of standard error in the linear scale to the mean of all data $\hat{v}_i$;

$$\omega = \left( \mathrm{e}^{s_L} - \mathrm{e}^{-s_L} \right) / 2 \tag{26}$$

$\omega$ and $s_L$ are almost equal because usually $s_L < 0.2$ (in which case their difference error is of the order of ${s_L}^3/3$, i.e., $\leq 0.008$, as can be checked by Taylor series expansions). Note that, although the approximate equality of $s_L$ and $\omega$ requires fitting in the scale on natural logarithm, $\ln v_c$, Figs. 11–13 are plotted, for convenience, in terms of the decadic logarithm, $\log v_c$.

The choice of beam sizes for testing has been governed by funding limitations and other subjective considerations. Unfortunately, the data points are crowded in the range of small sizes ($d \leq 20$ inches, Fig. 1 and 2). This distorts the resulting fit, giving insufficient weight to large beam data which are the most important for extrapolation to still larger sizes that could be used in practice. Ideally, the histogram of a database should be a horizontal line, but it is debatable whether this should be the case in the scale of $d$ or $\log d$. Therefore, two types of histogram-based data weighting are considered. In the fist type, the range of $d$ was divided into constant intervals, of 10 in. width, and the resulting histogram, plotted in Fig. 11 (bottom right), was approximated by the smooth curve plotted. Each point in the database was then assigned a weight inversely proportional to the smoothed histogram (because this is

(but this was advantageous for maximizing the brittleness number $\beta$); (2) that the beams were supposedly too narrow; and (3) that the bond slip was supposedly excessive (but so it was in many other tests, including those run in Toronto).

what is needed to make the weighted histogram a horizontal line in the scale of $d$). In the second type, the range of $\log d$ was divided into constant intervals, of width $\log 2$. The resulting histogram, shown in Fig. 12 (bottom right), was not approximated by a smooth curve but was used directly to assign to each point of the database a weight inversely proportional to this histogram.

To provide additional safety margin, the curve of design formulas has generally been made to pass not through the middle of the scatter band but near its lower margin. This provides an additional safety margin, imposed in addition to that provided by the load factors, by the capacity reduction factor, and by the fact that $f'_c$ is defined as a significantly smaller value than the mean compression strength from testing. To avoid bias, this additional safety margin must be obtained according to the least-square method—by taking the prediction formula obtained by least-square regression (solid curves in Figs. 11 and 12) and reducing it by the standard error of regression times a factor corresponding to the chosen probability cut-off, to be taken from the gaussian distribution table (which yields the dashed curves in Figs. 11 12).

In view of the large scatter of the database (Fig. 2), it is impossible to identify all the 9 parameters, $c_0, k_0, r_1, ...r_7$ without high uncertainty. Because the fitting of the available database has shown extremely small sensitivity to exponents $r_4, r_5, r_6$ and $r_7$, it was simply assumed that $r_4 = r_6 = r_7 = 0$ and $r_5 = 1/2$ (the exponent of 1/2 was chosen simply to agree with the current ACI design formula, $v_c \approx 2\sqrt{f'_c}$, motivated by Pauw's [57] observation that the tensile strength is approximately proportional to $\sqrt{f'_c}$).

As for the shear span $a/d$, although its effect should in principle be significant, the sensitivity to exponent $r_3$ is low, because of high scatter of the database. Therefore, two smooth formulas, one without $a/d$ and one with it, have been identified.

The simpler formula not involving $a/d$, which is the number one proposal for the code made here and is plotted in Fig. 11 (top left), reads:

$$\boxed{v_c \;=\; \frac{\mu\sqrt{f'_c}}{\sqrt{1 \,+\, d/d_0}}, \qquad d_0 = 1120 \left(\frac{\rho}{f'_c}\right)^{2/3}} \tag{27}$$

where

$$\mu = 5 \text{ (mean)}, \;\; \mu = 3.8 \text{ (design)} \qquad (s_L = 16.1\%, \omega = 16, 2\%) \tag{28}$$

($v_c$ and $f'_c$ are in psi, and $\rho$ is a number (not a percentage). The value $\mu = 5$ gives the solid curve in Fig. 11, representing the least-square fit (mean fit) of the database, while the value $\mu = 3.8$ gives the dashed curve in Fig. 11, which is obtained as the mean curve minus $1.65 s_L$ and corresponds to a 5% probability cut-off, i.e., the probability of $v_c$ lying below the dashed curve is 5% (the optimized values of all parameters are rounded off to the extent that $\omega$ would not be appreciably affected).

If the shear-span is included in the optimized formula, one gets a slightly more general formula, which is plotted in Fig. 11 (top right) and has the same form as (27) except that the values of $d_0, \mu, s_L$ and $\omega$ are replaced by:

$$d_0 = 1350 \left(\frac{\rho}{f'_c}\right)^{2/3} \left(\frac{d}{a}\right)^{1/3} \quad \text{with } \mu = 5.5 \text{ (mean)}, \;\; \mu = 4.2 \text{ (design)} \quad (s_L = 16.0\%, \omega = 16.0\%) \tag{29}$$

However, as seen from the $\omega$ value, the improvement achieved by considering $a/d$ is negligible.

Even though unsmooth formulas generally impair the convergence of computer algorithms (important, for example, for optimization of design), there has been a preference to use for codes straight-line formulas, possibly with inequality cut-off. In this spirit, the formula in Fig. 11 (bottom left) (having, not surprisingly, an appreciably higher coefficient of variation), has been obtained (with $D_0$ in inches);

$$\boxed{v_c \;=\; \min\left(\; \mu\sqrt{f'_c D_0/d}\;,\;\; \mu'\sqrt{f'_c}\;\right), \quad D_0 \;=\; 7\;\rho^{2/3}} \tag{30}$$

with $\mu = \mu' = 3.5$ (mean), $\mu = 2.5$ (design) $\qquad (s_L = 21.3\%, \omega = 21.5\%)$ (31)

Although $\mu'$ should equal $\mu$ from the statistical viewpoint, one could alternatively use for design $\mu' = 2$, in which case the current shear strength $2\sqrt{f'_c}$ would be retained for small enough sizes.

Fig. 11 shows dimensionless plots comparing the foregoing three formulas to the ACI-445 database, in which the area of each plotted data circle is proportional to the weight assigned on the basis of the histogram in $d$.

Fig. 12 gives analogous formulas obtained when the weights are assigned according to the histogram in $\log d$. The difference in fits is insignificant. For the sake of comparison, Fig. 13 gives analogous formulas obtained when all the points of the database have equal weights. Here the difference in fits compared to Fig. 12 is more pronounced and, especially, the data points for the deepest beams, which are the least numerous, are fitted poorly. Yet, a close fit of these data points is most important for extrapolation to larger sizes than tested.

Admittedly, the coefficients of variation $\omega$ of all the formulas are quite large, but this is due to the enormous data scatter. When the contamination by non-size parameter is eliminated, the scatter is far less; see Figs. 7–9.

The fact that the optimized exponent of steel ratio is positive calls for a comment. One might take the viewpoint [45] that small enough $\rho$ must lead to flexural failure due to yielding of steel, which is not brittle and corresponds to $d_0 \to \infty$. This viewpoint suggests that an increase of $\rho$ should cause an increase of brittleness, and thus should cause a decrease of $d_0$; in other words, the exponent of $\rho$ may be expected to be negative. Yet fitting of the database clearly indicates a positive exponent. The reason may be either that the database is spoiled by mixing too many influences, or that the viewpoint of transition to flexural failure is not germane. On the other hand, since high-strength concrete is more brittle than normal concrete and higher brittleness corresponds to smaller $d_0$, it is logical that the optimized exponent of $f'_c$ in the expression for $d_0$ is negative [45].

## Critical Examination of Other Formulas for Beam Shear

The close agreement with the broad-range Northwestern tests and Toronto tests (Fig. 7) and with the record-size Japanese tests (Fig. 8), together with the lack of disagreement with the classical size-effect tests (Fig. 9) of limited size ranges or small maximum sizes, provides strong experimental support for the fracture mechanics size effect espoused in this study, as well as a strong argument against other size effect formulas in beam shear which cannot fit these tests closely. Two among the other formulas, namely the CEB-FIP formula, and the power law of the type $v_c \propto d^{-1/3}$, are purely empirical and thus there is nothing to discuss beyond statistical comparisons with individual size-effect test series (regarding $v_c \propto d^{-1/3}$; see the curves in Figs. 7

(left and right) and 8, and regarding CEB-FIP, see Fig. 2). Theoretical justifications, however, have been proposed for three other formulas, which will now be discussed.

**1) Formula of Japan Society of Civil Engineers (JSCE)**

As a consequence of a pioneering proposal of Oakamura and Higai [55] made in 1980 (several years before the onset of the energetic fracture-based theory), and of a later recalibration in [53, 54], a power law of the type $v_c \propto d^{-1/4}$ (proposed on an empirical basis already by Kani [44]) was adopted for the concrete design code in Japan [43]. In 1980, Okamura and Higai's proposal was a breakthrough and it was logical to underpin it by Weibull's (1939) statistical theory, the only size effect theory available at that time. That theory [24] indicates a power law size effect with exponent $-3/m$ for three-dimensional similarity and $-2/m$ for two-dimensional similarity, where $m$ is the empirical Weibull modulus (shape parameter), the value of which is normally determined from the coefficient of variation of tensile strength of many identical specimens. Based on the classical work of Zech and Wittmann [68], Okamura and Higai assumed that $m = 12$. Further assuming three-dimensional similarity to apply, they came up with the exponent $-3/m = -1/4$.

Recent in-depth studies [18, 19, 20], however, showed that the apparent value of $m$ for concrete increases markedly with structure size and that, after separation of deterministic nonlocal effects, the correct value of Weibull modulus for concrete is about $m \approx 24$. This gives, for three-dimensional similarity, the exponent $-3/m = -1/8$.

Furthermore, it transpired that not only the exponent value but also the assumption of three-dimensional similarity of beam shear failures needs to be revised. The reason is that material failure at one point in three dimensions does not suffice to ruin the beam. Rather, the beam must fail simultaneously over its whole width, which means that the location of the failure initiation point could be random only in two dimensions (in the length and depth coordinates, but not in the width coordinate). Therefore, if the Weibull theory were applicable, the size effect exponent would have to be $-2/m = -1/12$. This gives in the bi-logarithmic plot a straight line of slope $-1/12$ rather than $-1/4$. But such a weak size effect blatantly disagrees with all the test data. This confirms that the Weibull theory cannot be applied to the mean size effect in the beam shear problem (however, if extended to a nonlocal form, it nevertheless appears applicable to the random scatter [13]).

Furthermore, as gradually established, the assumption that the shear failure of reinforced concrete beams is governed by Weibull statistical theory is itself fundamentally unacceptable. That theory is predicated on the hypothesis that the failure occurs as soon as a macroscopic crack initiates from one microscopic flaw, before any significant stress redistribution in the structure is caused by the fracture process. This is true for fatigue fracture of metals or fine-grained ceramics, but not concrete (except perhaps on the scale of a large dams, the cross section of which is far larger than the characteristic length $l_0$ of the fracture process zone in concrete, which is typically 0.5 m). The beam does not fail at the initiation of diagonal shear crack, as would be required by Weibull theory, but only after this crack has propagated in a stable manner through most of the cross section. The growth of the main diagonal shear crack is governed primarily by redistribution of the mean (deterministic) stress field. The randomness of the local strength of concrete at points located far away from the crack path dictated by fracture mechanics cannot significantly deflect that path. Therefore, the mean size effect observed in beam shear failure is caused predominantly by deterministic stress redistribution and the associated energy release prior to failure. The statistical contribution described by Weibull's

statistical theory is negligible for the mean response [18, 19, 20, 11, 22, 12], although it doubtless influences the scatter.

Weibull's statistical size effect, which is much milder than the energetic size effect associated with stress redistribution, is applicable to the first cracking load. That this size effect exists, and that it is indeed much weaker than the size effect on nominal strength, is confirmed, e.g., by the test data in Fig. 4 in [63].

### 2) Crack Spacing Theory and Role of Cohesive Stresses Across the Crack

The maximum crack opening width $w$ is roughly proportional to effective crack spacing $s_e$, while $s_e$ is roughly proportional to $d$. Hence, the deeper the beam, the larger is $w$ at maximum load. The larger the crack width, the smaller are the cohesive stresses $\sigma_1$ transmitted across the diagonal shear crack. These facts are indisputable. However, it was proposed [65, 32] that the reduction of the cohesive stresses with increasing $d$ should be the physical source of size effect. This proposition, which they incorporated into their modified compression field theory (MCFT), is untenable.

In this theory, it is assumed that $v_c$ decreases with $w$ as $v_c = \text{constant}/(1 + c_1 w)$ where $c_1$ is a parameter depending on the maximum aggregate size. Assuming $w$ to be approximately proportional to $s_e$, one gets the relation $v_c = v_0/(1 + c_0 s_e)$ where $v_0, c_0$ are certain constants. Considering beams with no stirrups and no horizontal steel bars other than those at the bottom, and assuming $s_e$ to be proportional to $d$ [31], one gets for the MCFT crack spacing theory of size effect a formula of the type:

$$v_c \;=\; \frac{v_0}{1 \,+\, d/d_0} \tag{32}$$

where $d_0$ and $v_0$ are parameters independent of structure size. For $d \gg d_0$, this formula approaches the final asymptotic size effect $v_c \propto d^{-1}$ (which is sketched by the dashed lines in Fig. 2). Although the coefficients of the formula are set up so that the test data would lie in the transitional range between the horizontal and inclined asymptotes in the log-log plot, in which the formula gives a much milder slope than $-1$ and can match some of the existing data [31], the asymptotic size effect $d^{-1}$ (proposed by Leonardo da Vinci [35] and disputed by Galileo [38]) is theoretically objectionable and in fact thermodynamically impossible (exponent $-1/2$ is the strongest size effect possible). This observation suffices to conclude that the crack spacing theory does not have a sound theoretical basis. But there are more practical objections.

Finite element simulation of propagation of a diagonal shear crack according to the cohesive (or Hillerborg's, fictitious) crack model [39] shows that, if the concrete is assumed to have an unlimited compression strength, the load-deflection diagram is always rising, i.e., has no peak; see Fig. 10e. Therefore, the stresses transmitted across the diagonal shear crack cannot decide the maximum load, contrary to what is assumed in the crack spacing theory. Rather, the maximum load must be controlled by the shear-compression fracture of the ligament above the tip of the diagonal shear crack (Fig. 10e). This conclusion is supported by the fact that the compression stresses in the ligament attain the compression strength of concrete (which in turn implies that, in the strut-and-tie model, the failure must be decided by the crushing of the compression strut [9, 12]). So the size effect in beam shear physically represents the size effect of shear-compression fracture.

The fact that the cohesive stresses across a diagonal shear crack cannot have a significant influence on the maximum load is further supported by the experimental observations at the University of Toronto [1, 31]. Fig. 10a,b shows the major cracks observed near the maximum load. The strain in the steel bar at the cross section passing through the tip of the main

diagonal shear crack was also measured. From this, one can calculate the axial force in the steel, and knowing this force and the bending moment, one can find the precise location of the compression force resultant in this cross section of the tested beam (Fig. 10b). Because this resultant must also pass through the point of intersection of steel bars and the vertical resultant at the support, one readily identifies the line of the compression resultant, which is drawn in Fig. 10b.

Now it should be noted that this resultant passes above the observed main diagonal crack and runs parallel to the top segment of this crack. Consequently, the shear and normal stresses transmitted across that crack at maximum load must be negligible. From the magnitude of this resultant one can also estimate the compression stresses $\sigma_2$ in the ligament above the crack tip. One finds them to be roughly equal to the compression strength of concrete, $f'_c$. Because the tensile cohesive stresses $\sigma_1$ in the diagonal crack at maximum load must be much less than the tensile strength $f'_t$ (surely less than $0.5f'_t$), and because $f'_t \approx 0.1f'_c$, it follows that $\sigma_1$ must be less than $0.05\sigma_2$, probably much less. So it must be concluded that the contribution of the tensile cohesive stresses $\sigma_1$ in the diagonal crack at maximum load must be negligible compared to the contribution of the compressive stresses $\sigma_2$ parallel to the crack (Fig. 10d), and thus cannot control the maximum load. This conclusion puts again in question the physical explanation of size effect by the crack spacing theory [32, 65].

The fact that the line of the compression resultant as identified in Fig. 10 is parallel to the end portion of the diagonal shear crack (or that it does not intersect this crack) further implies that shear stresses due to aggregate interlock cannot have an important effect on the maximum load.[10]

### Fractal Characteristics of Fracture and Carpinteri's MFSL

The role of the fractal characteristics of fracture has been debated for almost a decade, and a clearer picture is gradually emerging [62]. Although some questions remain unresolved [25], two salient points crystallized:

(1) The so-called 'multi-fractal scaling law' (MFSL) proposed by Carpinteri [30] cannot be applied to failures occurring after large stable crack growth, which is the case of diagonal shear cracks in beams, the main reason being that the stress redistribution due to large cracks and the associated energy release are not taken into account in the existing form of the fractal theories.

(2) The MFSL is identical to a special case of a more general size effect formula for crack initiation derived from (non-fractal) fracture mechanics [16, 17] and refined in [7] (see also [8, 12]). So there is no longer any disagreement about the formula itself, but only about the physical justification of the formula [62, 25]. Because this formula deals only with failures at crack initiation (e.g., modulus of rupture), there is no need to dwell on the difficult fractal questions any more. They are not relevant to our problem.

[10] Also note that, in the strut-and-tie (truss) model, the straight line connecting the support and the applied load (of slope $a/d$) would normally be assumed as the axis of the imagined 'compression strut'. The fact that the Toronto measurements imply a much steeper compression resultant means that the simplistic version of the strut-and-tie model (or truss model) is invalid. While the fracturing strut-and-tie model [9] can explain the size effect in beam shear, uncertainty about the correct slope of the compression strut in beam shear remains to be one obstacle to using the strut-and-tie model as a predictive tool.

## Conclusions

1. Because the size range of main practical interest lies outside the range of the available test data, the size effect law cannot be set up purely empirically. A realistic theoretical foundation is inevitable.

2. Since concrete is just one of many quasibrittle materials failing due to quasibrittle fracture or softening damage, it would be illogical to expect different laws to govern failure. Laws that are common to all these materials are a more logical choice, especially when the experimental evidence is ambiguous due to high random scatter.

3. The hypothesis that the maximum load in shear failure is controlled by propagation of cohesive fracture or softening damage leads to the same size effect law as established for other quasibrittle materials. The experimental evidence can be matched with this law as closely as one could desire in view of the inevitable experimental scatter.

4. Although a specialized fracture-based model, such as the fracturing truss model, yields a realistic form of the size effect formula and intuitively explains the mechanism of size effect, this model is insufficient for predicting the dependence of size effect law coefficients on the shear span, reinforcement ratio, aggregate size, material strength, etc.

5. In the asymptotic situations of infinitely small and infinitely large structures, the analysis of failure and size effect becomes far simpler and clearer than in the practical size range. Therefore, it is appropriate to derive a theoretical formula by asymptotic matching, a technique that 'interpolates' between the known asymptotic behaviors at the opposite infinities.

6. Assuming the failure load to be controlled by cohesive fracture parameters (material strength $\sigma_0$ and fracture energy $G_f$), and exploiting the known first two asymptotic terms of the large- and small-size asymptotic expansions of the cohesive crack model (or the nonlocal damage models), one can easily deduce a simple transitional size effect law by means of dimensional analysis.

7. Asymptotic matching based on dimensional analysis leads logically to the size effect law proposed for beam shear by Bažant in 1994. As a simplification, one can also use a power law of exponent $-1/2$, supplemented with an upper bound for small sizes.

8. The size effect law established agrees with all of the existing test series in which the beam depth was varied significantly, the number of which is 11. Especially, this size effect law agrees with the tests conducted at Northwestern University and at University of Toronto, which represent the only data with a broad size range and almost perfect geometrical scaling.

9. Most importantly, the Northwestern and Toronto test series, and the Japanese tests of Shioya et al. (which are the only scaled tests of a significant size range) confirm that the large-size asymptotic slope of size effect is $-1/2$. This in turn proves that the explanation of failure lies in fracture mechanics.

10. The coefficients of the size effect law are calibrated by optimum fitting of the ACI-445 database (which includes 398 data) and of the Northwestern University database (664 data) [29]. However, since these large databases are inevitably contaminated by random

variation of factors other than the size, the differences in the coefficients of variation of errors in comparison to other proposed formulas are relatively insignificant.

11. The size effect law in (27) provides a good and simple representation of the ACI-445 database. The coefficient of variation of regression errors, which is about 16%, allows determining the 5% probability cut-off which is suitable for a design code formula.

12. Comparisons with the required asymptotic behavior and with the test data pertinent to the size effect in beam shear reveal serious contradictions with the old theories and formulas (including the JSCE formula based on Weibull statistical theory, the crack spacing enhancement of MCFT, the empirical CEB-FIP formula, and the application of MFSL to diagonal shear failure) and reveal significant disagreement with the empirical power law of exponent $-1/3$.

**Acknowledgment:** *Financial support by the Infrastructure Technology Institute of Northwestern University is gratefully acknowledged. Professor M.T. Kazemi of Sharif University of Technology, Tehran, is thanked for valuable comments.*

## Appendix I. The Question of Difference Between Notched Specimens and Unnotched Structures with Large Cracks

Application of the size effect law (17) to unnotched structures with large cracks rests on two hypotheses:

*Hypothesis I.* The major cracks at failure in small and large structures are geometrically similar.

*Hypothesis II.* The fracture process zones at the tips of a notch or a crack give approximately the same energy dissipation rates.

According to the cohesive (or fictitious) crack model, both hypotheses are asymptotically exact for $d \to \infty$ and thus are good approximation for large enough beams. These hypotheses are justified by the following theorem: *As long as the fracture problem has a unique solution, sharp (LEFM) cracks in geometrically similar structures have similar paths and, at maximum load (as well as other corresponding stages of loading), also geometrically similar lengths.* This theorem can be rigorously proven by scaling transformations of all the differential equations, boundary conditions and crack face conditions of equivalent LEFM, which is an approximation (widely used in nonlinear fracture mechanics) based on the assumption that a crack with a large fracture process zone is approximately equivalent to a sharp (LEFM) crack with a tip located in the middle of the fracture process zone.

The cohesive crack model shows that the cohesive stress $\sigma_{tail}$ at the tail of the fracture process zone is zero for a naturally growing crack. But when the fracture process zone is attached to the notch tip, $\sigma_{tail}$ is, for a finite beam size, non-zero (approaching zero only if the size tends to infinity). The consequence is that the size effect with second-order asymptotic accuracy for large sizes is slightly different from (17):

$$v_c = v_0 \left( \frac{d_1}{d_1 + d} + \frac{d}{d_0} \right)^{-1/2} \tag{33}$$

(see [11], and in detail Eqs. 9.77 and 9.109 in [12]). Here $d_0$ and $d_1$ are constants, and $d_1$ must be larger than $d_0$. Obviously this law has the same asymptotes as (17) (which is of course required by the dimensional analysis presented here) and for $d_1 \to \infty$ becomes identical to (17).

For finite $d_1$, the transition between the asymptotes is more abrupt (with a sharper curvature) than for (17), and the $v_c$ values in the intermediate range are always larger. But they are only slightly larger. Based on preliminary numerical cohesive crack simulations, $d_1 \approx 5d_0$ to $10d_0$, but then the difference from (17) is negligible compared to the uncertainty due to the scatter of test results. This is one justification of the use the simpler size effect law (17) for beam shear. Besides, (33) has one more unknown parameter than (17), and the data scatter makes it next to impossible to identify it experimentally.

Another justification stems from the fact that, before an overload to failure, the beam may be subjected to cyclic loading. Such loading reduces the cohesive stresses in a naturally grown crack to almost zero, which means that a preexisting fatigued crack is stress free and thus acts like a notch. Assuming that cyclic loading may occur is on the side of safety.

Finally, those who think that the difference between a notch and a natural crack is important should note that the growth of the diagonal shear crack is usually not what causes the load to peak. Rather, it is the growth of shear-compression fracture across the ligament above the tip of the diagonal shear crack. How the difference between a notch and a naturally grown crack might affect such fracture is not known. But the present asymptotic considerations based on dimensional analysis, which led to (17), must apply to shear-compression fracture as well.

## Appendix II. Questions of Statistical Evaluation and Bias

Although formula identification from beam shear data is a problem of statistical regression, in one current (unpublished) investigation it has been tried to reduce comparisons of various proposed formulas for beam shear to elementary population (ensemble) statistics of the ratios $\gamma_i$ of the measured and calculated values. In this investigation, the coefficient of variation has been defined as follows:

$$\text{COV}^* \;=\; \frac{1}{\bar{\gamma}}\sqrt{\frac{1}{n-1}\sum_i(\gamma_i-\bar{\gamma})^2} \quad \text{with} \quad \bar{\gamma} \;=\; \frac{1}{n}\sum_i \gamma_i \tag{34}$$

$$\text{where} \qquad \gamma_i = \hat{v}_i/v_i \qquad (i=1,2,...n) \tag{35}$$

However, such an approach is fundamentally incorrect, for four reasons. First, if the parameter identification is not based on the method of least squares, the results cannot be unbiased, i.e., the resulting mean and variance of formula parameters cannot be the mean and variance of the statistical distribution of these parameters. Second, if the minimized expression is not a sum of squares of errors, the tangential linearizations made in any data fitting algorithm can lead to numerical instability. Third, fitting of the ratio $\hat{v}_i/v_i$ implies weighting of the data $\hat{v}_i$ as a function of the unknown values of $v_i$ to be solved, which is inadmissible. Fourth, if all $v_i$ in (35) and (34) are replaced by $kv_i$, $k$ being any constant between $-\infty$ and $\infty$, then $\gamma_i$ and $\bar{\gamma}_i$ are replaced by $\gamma_i/k$ and $\bar{\gamma}_i/k$, and so it is found that the value of $\text{COV}^*$ does not change. Such a definition of the coefficient of variation, which is insensitive to multiplying the formula for $v_c$ by any number, makes no sense at all. Obviously, minimization of $(\text{COV}^*)^2$ cannot be used to calibrate formula parameters.

As a workable alternative to the use of ratios $\gamma_i = \hat{v}_i/v_i$, it has bee tried to identify formula parameters by minimizing not $(\text{COV}^*)^2$ but the sum $\Phi = \sum_i(\gamma_i - 1)^2$. This sum may be rewritten as:

$$\Phi = \sum_{i=1}^{n}\left(\frac{\hat{v}_i}{v_i}-1\right)^2 = \sum_{i=1}^{n} w_i(\hat{y}_i - y_i)^2 \tag{36}$$

$$\text{where} \qquad y_i = 1/v_i, \quad \hat{y}_i = 1/\hat{v}_i, \quad w_i = (\bar{v}_i)^2 \tag{37}$$

So, the minimization of $\Phi$ represents simply a weighted least-square regression of data $\bar{y}_i$, minimizing the sum of squared errors in $y_i$ with weights $w_i$ proportional to the squares of the measured values $\hat{v}_i$. Aside from a misguided desire to avoid regression statistics, the motivation for use of the ratios $\gamma_i = \hat{v}_i/v_i$ has been to increase the weight of smaller $v_i$ values. But there is a problem with this motivation. As is well known [37, 2, 52, 36, 27, 59, 49], to minimize bias, the regression should be conducted in such variables in which the variance ($\mathrm{Var}(v_c|d)$, in our case) is as uniform as possible, and nonuniform weights should not be used unless the variance varies by an order of magnitude or more (i.e., if the data are heteroskedastic). For beam shear size effect data (as well as most size effect data), the variance appears to be the least nonuniform in the plots of $\log v_c$ versus $\log d$, and so these are the preferable coordinates for statistical regression. The implication of unjustified shear strength dependence of the weights in (37) is that the minimization of (36) is not unbiased, i.e., the estimates of the mean and the standard deviation (or COV) of the optimized parameters are not the actual mean and standard deviation of the statistical distribution of these parameters (in other words, are not the 'maximum likelihood' estimates). One consequence is that the mean plus 1.65 times standard deviation does not give the correct (unbiased) value for the 5th percentile, needed for setting up the design formula, and generally all the statistical estimates are not correct (note that data weighting to compensate for the crowding of data points into the small-size range is an entirely different matter). On the other hand, the absence of shear-strength dependent weighting from the least-square fitting of $\ln v_c$ ensures that the optimized parameters are unbiased. Because $(\mathrm{d}(v_c)^2 = (\mathrm{d}v_c)^2/(v_c)^2$, the transformation of scale from linear to logarithmic has a similar effect as the weighting of the data in proportion to $1/(v_c)^2$, but without causing any statistical bias.

# References


[1] Angelakos, D, Bentz, E.C., and Collins, M.P. (2001). "Effect of concrete strength and minimum stirrups on shear strength of large members." *ACI Structural J.* 98 (3), 290–300.

[2] Ang, A. H.-S., and Tang, W.H. (1976). *Probability concepts in engineering planning and design.* Vol. 1, Sec.7.

[3] Bahl, N.S. (1968) *Über den Einfluss der Balkenhöhe auf Schubtragfähighkeit von einfeldrigen Stalbetonbalken mit und ohne Schubbewehrung.* Dissertation, Universität Stuttgart.

[4] Barenblatt, G.I. (1962). "The mathematical theory of equilibrium of cracks in brittle fracture." *Adv. Appl. Mech.*, 7, 55–129.

[5] Bažant, Z.P. (1984). "Size effect in blunt fracture: Concrete, rock, metal." *J. of Engrg. Mechanics*, ASCE, 110, 518–535.

[6] Bažant, Z.P. (1987). "Fracture energy of heterogeneous material and similitude." Preprints, *SEM-RILEM Int. Conf. on Fracture of Concrete and Rock* (held in Houston, Texas, June 1987), ed. by S. P. Shah and S. E. Swartz, publ. by SEM (Soc. for Exper. Mech.) 390–402.

[7] Bažant, Z.P. (1998). "Size effect in tensile and compression fracture of concrete structures: computational modeling and design." *Fracture Mechanics of Concrete Structures* (Proc., 3rd Int. Conf., FraMCoS-3, held in Gifu, Japan), H. Mihashi and K. Rokugo, eds., Aedificatio Publishers, Freiburg, Germany, 1905–1922.

[8] Bažant, Z.P. (1991). "Why continuum damage is nonlocal: Micromechanics arguments." *Journal of Engineering Mechanics* ASCE 117 (5), 1070–1087.

[9] Bažant, Z.P. (1997). "Fracturing truss model: Size effect in shear failure of reinforced concrete." *J. of Engrg. Mechanics* ASCE 123 (12), 1276–1288.

[10] Bažant, Z.P. (1999). "Size effect in concrete structures: nuisance or necessity?" (plenary keynote lecture), in *Structural Concrete: The Bridge Between People, Proc.,* fib *Symp. 1999* (held in Prague), Fédération Internationale du Béton, publ. by Viacon Agency, Prague, pp. 43–51.

[11] Bažant, Z.P. (2001). "Probabilistic modeling of quasibrittle fracture and size effect." (principal plenary lecture, Proc., 8th Int. Conf. on Structural Safety and Reliability (ICOSSAR), held at Newport Beach, Cal., 2001), R.B. Corotis, ed., Swets & Zeitinger (Balkema), 1–23.

[12] Bažant, Z.P. (2002). *Scaling of structural strength.* Hermes–Penton, London.

[13] Bažant, Z.P. (2003). "Statistical distribution of size effect in quasibrittle fracture." Report, in preparation.

[14] Bažant, Z.P., and Kazemi, M.T. (1991). "Size effect on diagonal shear failure of beams without stirrups." ACI *Structural Journal* 88 (3), 268–276.

[15] Bažant, Z.P., and Kim, Jenn-Keun (1984). "Size effect in shear failure of longitudinally reinforced beams." *Am. Concrete Institute Journal*, 81, 456–468; Disc. & Closure 82 (1985), 579–583.

[16] Bažant, Z.P., and Li, Z. (1995). "Modulus of rupture: size effect due to fracture initiation in boundary layer." *J. of Struct. Engrg.* ASCE, 121 (4), 739–746.

[17] Bažant, Z.P., and Li, Z. (1996). "Zero-brittleness size-effect method for one-size fracture test of concrete." *J. of Engrg. Mechanics* ASCE 122 (5), 458–468.

[18] Bažant, Z.P., and Novák, D. (2000). "Energetic probabilistic size effect, its asymptotic properties and numerical applications." *Proc., European Congress on Computational Methods in Applied Science and Engineering (ECCOMAS 2000 )*, Barcelona, pp. 1–9.

[19] Bažant, Z.P., and Novák, D. (2000a). "Probabilistic nonlocal theory for quasibrittle fracture initiation and size effect. I. Theory." *J. of Engrg. Mech.* ASCE 126 (2), 166–174.

[20] Bažant, Z.P., and Novák, D. (2000b). "Probabilistic nonlocal theory for quasibrittle fracture initiation and size effect. II. Application." *J. of Engrg. Mech.* ASCE 126 (2), 175–185.

[21] Bažant, Z.P., and Novák, D. (2000c). "Energetic-statistical size effect in quasibrittle failure at crack initiation." *ACI Materials Journal* 97 (3), 381–392.

[22] Bažant, Z.P., and Novák, D. (2001). "Proposal for standard test of modulus of rupture of concrete with its size dependence." *ACI Materials Journal* 98 (1), 79–87.

[23] Bažant, Z.P., and Oh, B.-H. (1983). "Crack band theory for fracture of concrete." *Materials and Structures* (RILEM, Paris) 16, 155–177.

[24] Bažant, Z.P., and Planas, J. (1998). *Fracture and Size Effect in Concrete and Other Quasibrittle Materials.* CRC Press, Boca Raton and London (Sections. 9.2, 9.3)

[25] Bažant, Z.P., and Yavari, H. (2003). "Should the size effect in quasibrittle structures be modeled by multifractal or energetic scaling law?" *Theor. and Appl. Mech. Report* Northwestern University (in preparation).

[26] Bažant, Z.P., Yu, Q., and Zi, G. (2002). "Choice of standard fracture test for concrete and its statistical evaluation." *Int. J. of Fracture* 118 (4), Dec., 303–337.

[27] Beck, J.V., and Arnold, K.J. (1977). *Parameter estimation in engineering science.* J. Wiley, New York.

[28] Buckingham, E. (1914). "On Physically Similar Systems: Illustrations of the Use of Dimensional Equations." *Phys. Rev.* 4, 345-376.

[29] Becq-Giraudon, E. (2000). "Size effect on fracture and ductility of concrete and fiber composites" *Ph.D. Dissertation*, Northwestern University.

[30] Carpinteri, A. (1994). "Fractal nature of materials microstructure and size effects on apparent material properties." *Mechanics of Materials* 18, 89–101.

[31] Collins, M.P., and Kuchma, D. (1999). "How safe are our large, lightly reinforced concrete beams, slabs and footings." *ACI Structural J.* 96 (4), 482–490.

[32] Collins, M.P., and Mitchell, D. (1991). "Prestressed concrete structures." Prentice Hall, Englewood Cliffs, New Jersey 1991 (section 7.10).

[33] Collins, M.P., Mitchell, S., Adebar, P. and Vecchio, F.J. (1996) "General shear design method." *ACI Struct. J.*, 93(1), 36–45.

[34] Comité Euro-international du Béton (1991) CEB-FIP Model Code 1990.

[35] da Vinci, L. (1500s)—see *The Notebooks of Leonardo da Vinci* (1945), Edward McCurdy, London (p. 546); and *Les Manuscrits de Léonard de Vinci*, transl. in French by C. Ravaisson-Mollien, Institut de France (1881-91), Vol. 3.

[36] Draper, N., and Smith, F. (1981). *Applied regression analysis.* 2nd ed. J. Wiley, New York.

[37] Fox, J. (1997). *Applied regression analysis, linear models and related methods.* Sage Publications (also: http://socser.socsci.mcmaster.ca/jfox/Books/Applied-Regression/in...).

[38] Galileo Galilei Linceo (1638) *Discorsi i Demostrazioni Matematiche intorno à due Nuove Scienze*, Elsevirii, Leiden. (English transl. by T. Weston, London (1730), pp. 178–181)

[39] Hillerborg, A., Modée, M. and Petersson, P.E. (1976). "Analysis of crack formation and crack growth in concrete by means of fracture mechanics and finite elements." *Cement Concrete Res.*, 6, 773–782.

[40] Iguro, M., Shioya, T., Nojiri, Y. and Akiyama, H. (1985) "Experimental studies on shear strength of large reinforced concrete beams under uniformly distributed load." *Concrete Library International of JSCE*, No.5 (translation from *Proceedings of JSCE*, No. 345/V-1, August 1984), 137–146.

[41] Irwin, G.R. (1958). "Fracture." In *Handbuch der Physik*, Vol. 6, Flügge, ed., Springer-Verlag, Berlin, pp. 551–590.

[42] Izquerdo-Encarnación, J.M. (2003). "Ars sine scientia nihil est." *Concrete International* 25 (5), May, p. 7.

[43] (1991). "Standard specification for design and construction of concrete structures. Part I (Design), Japan Soc. of Civil Engrs., Tokyo.

[44] Kani, G.N.J. (1967). "How safe are our large reinforced concrete beams?" *ACI J.*, 58(5), 591–610.

[45] Kazemi, M.T. (2003). Private communication to Z.P. Bažant.

[46] Kfouri, A.P., and Rice, J.R. (1977). "Elastic-plastic separation energy rate for crack advance in finite growth steps." *Fracture 1977* (Proc., 4th Int. Conf. on Fracture, ICF4, Waterloo), D.M.R. Taplin, Ed., Univ. of Waterloo, Ontario, Canada, Vol. 1, 43–59.

[47] Knauss, W.C. (1973). "On the steady propagation of a crack in a viscoelastic sheet; experiment and analysis. *The Deformation in Fracture of High Polymers*, H.H. Kausch, Ed., Plenum, New York 501–541.

[48] Knauss, W.C. (1974). "On the steady propagation of a crack in a viscoelastic plastic solid." *J. of Appl. Mech. ASME* 41 (1), 234–248.

[49] Lehmann, E.L. (1959). *Testing statistical hypotheses.* J. Wiley, New York.

[50] Leonhardt, F. and Walther, R. (1962) "Beiträge zur Behandlung der Schubprobleme in Stahlbetonbau." *Beton-und Stahlbetonbau* (Berlin), March, 54–64, and June, 141–149.

[51] Leonov, M.Y., and Panasyuk, V.V. (1959). "Development of a Nanocrack in a Solid." *Prikldnaya Mekhanika* (transl. Soviet Applied Mechanics) 5 (4), 391–401; English transl. in *Fracture: A topical encyclopedia of curent knowledge*, G.P. Cherepanov, ed., Krieger Publ. Co., Malabar, Florida 1998.

[52] Mandel, J. (1984). *The statistical analysis of experimental data.* Dover Publications.

[53] Niwa, J., Yamada, K., Yokozawa, K. and Okamura, M.P.S. (1986). "Reevaluation of the equation for shear strength of R.C. beams without web reinforcement." *Proceedings of the Japanese Society of Civil Engineers*, Vol. 5, No.372, 1986–1988.

[54] Niwa, J., Yamada, K., Yokozawa, K., and Okamura, H. (1987). "Reevaluation of the equation for shear strength of reinforced concrete beams without web reinforcement." *JSCE Concrete Library International* 9, 65–84.

[55] Okamura, H. and Higai, T. (1980). "Proposed design equation for shear strength of reinforced concrete beams without web reinforcement." *Proceedings of Japanese Society of Civil Engineers*, Vol. 300, 131–141

[56] Palmer, A.C. and Rice, J.R. (1973). "The growth of slip surfaces on the progressive failure of over-consolidated clay" *Proc. Roy. Soc. Lond. A.*, 332, 527-548

[57] Pauw, A. (1960). "Static modulus of elasticity of concrete as affected by density" *Journal of the American Concrete Institute.*, 32: 679–687

[58] Petersson, P.E. (1981). " Crack growth and development of fracture zones in plain concrete and similar materials." *Report* TVBM-1006, Div. of Building Materials, Lund Inst. of Tech., Lund, Sweden.

[59] Plackett, R.L. (1960). *Principles of regression analysis.* Clarendon Press.

[60] Riabouchinski D.P. (1911-12). Annual Report. *British Advisory Committee for Aeronautics*, Abstract No. 134, p. 260 (also *L'Aerophile*, Sept. 1, 1911).

[61] Rice, J.R. (1968). "Mathematical analysis in the mechanics of fracture", *Fracture—An advanced treatise*, Vol. 2, ed. H. Liebowitz, Academic Press, New York, 191–308.

[62] RILEM (2003) Committee QFS, "Quasibrittle Fracture Scaling." State-of-Art Report; to be submitted to *Materials and Structures* (RILEM).

[63] Shioya, T. and Akiyama, H. (1994). "Application to design of size effect in reinforced concrete structures." *Size Effect in Concrete Structures* (Proc., Japan Concrete Institute International Workshop, Sendai), H. Mihashi, H. Okamura and Z.P. Bažant, eds., E&FN Spon, London, 409–416.

[64] Smith, E. (1974). "The structure in the vicinity of a crack tip: A general theory based on the cohesive crack model." *Engineering Fracture Mechanics* 6, 213–222.

[65] Vecchio, F.J., and Collins, M.P. (1986). "The modified compression field theory for reinforced concrete elements subjected to shear." *ACI J.. Proc.* 83 (2), 219–231.

[66] Weibull, W. (1939). "A statistical theory of the strength of materials." *Proc. Royal Swedish Academy of Eng. Sci.* 151, 1–45.

[67] Wnuk, M.P. (1974). "Quasi-static extension of a tensile crack contained in viscoelastic plastic solid." *J. Appl. Mech. ASME* 41 (1), 234–248.

[68] Zech, B. and Wittmann, F.H. (1977). "A complex study on the reliability assessment of the containment of a PWR, Part II. Probabilistic approach to describe the behavior of materials." *Trans. 4th Int. Conf. on Structural Mechanics in Reactor Technology*, T.A. Jaeger and B.A. Boley, eds., European Communities, Brussels, Belgium, Vol. H, J1/11, 1–14.

# List of Figures

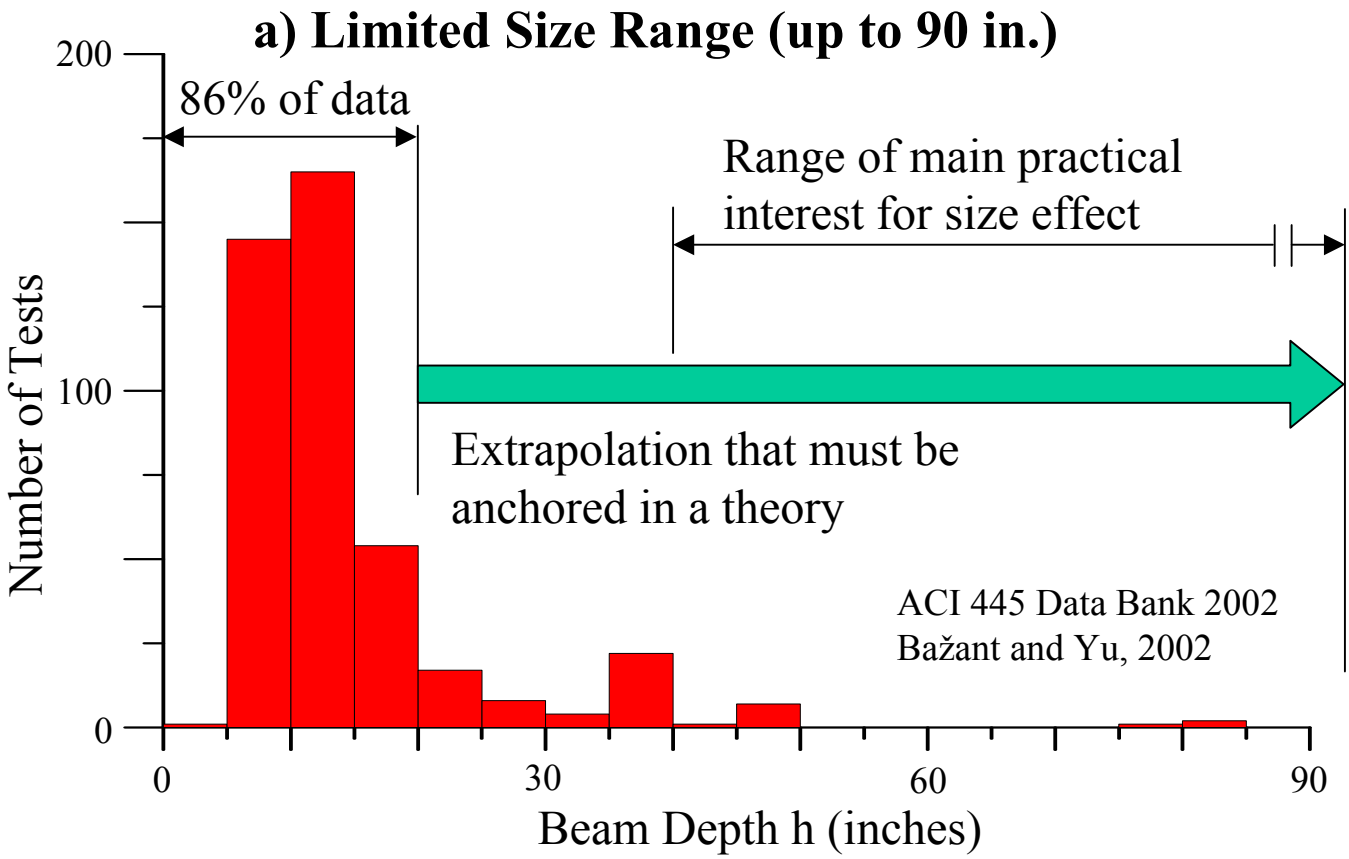
a) Limited Size Range (up to 90 in.)
200
100
0
Number of Tests
86% of data
Range of main practical
interest for size effect
Extrapolation that must be
anchored in a theory
ACI 445 Data Bank 2002
Bažant and Yu, 2002
0
30
60
90
Beam Depth h (inches)

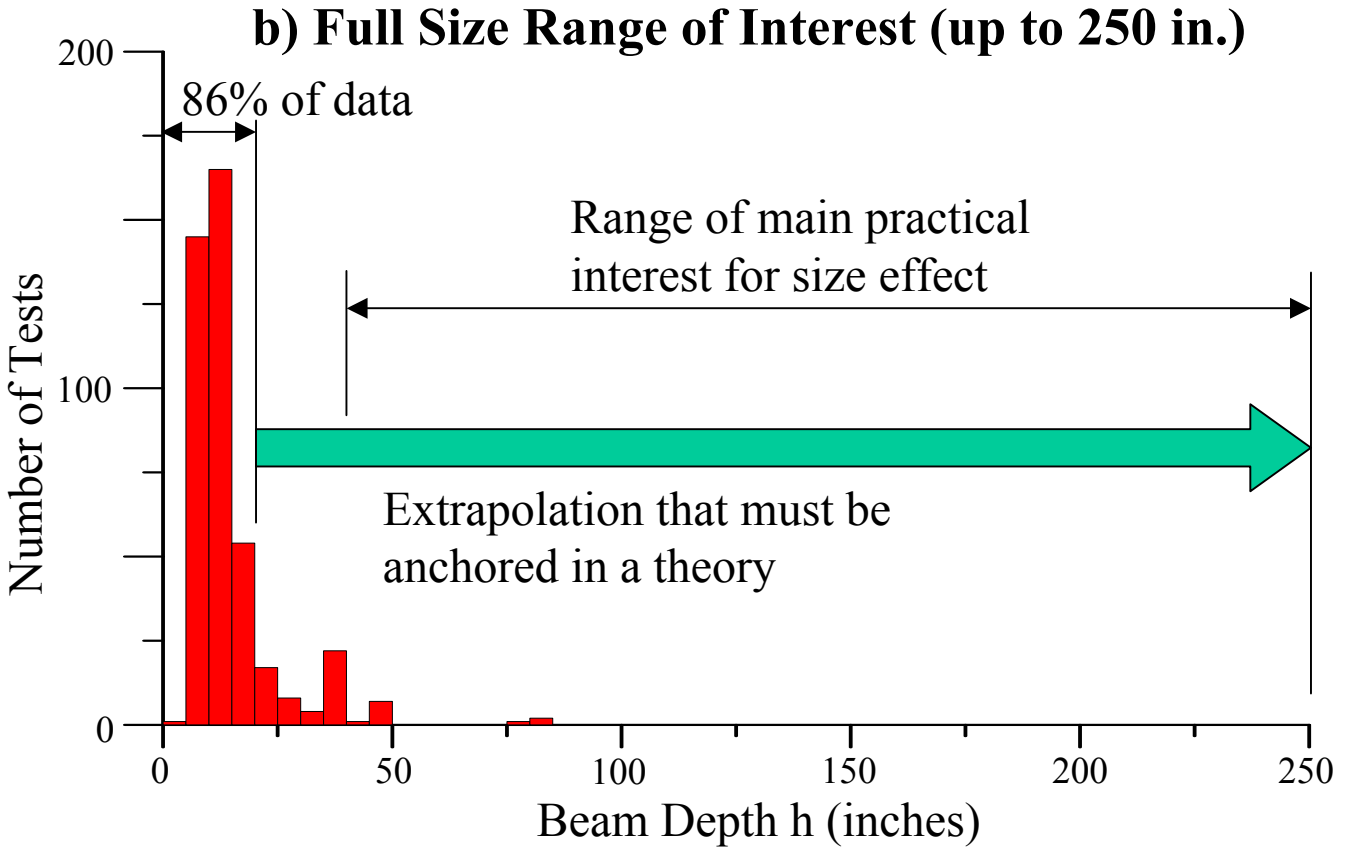
b) Full Size Range of Interest (up to 250 in.)
200
100
0
Number of Tests
86% of data
Range of main practical
interest for size effect
Extrapolation that must be
anchored in a theory
0
50
100
150
200
250
Beam Depth h (inches)

Fig. 1

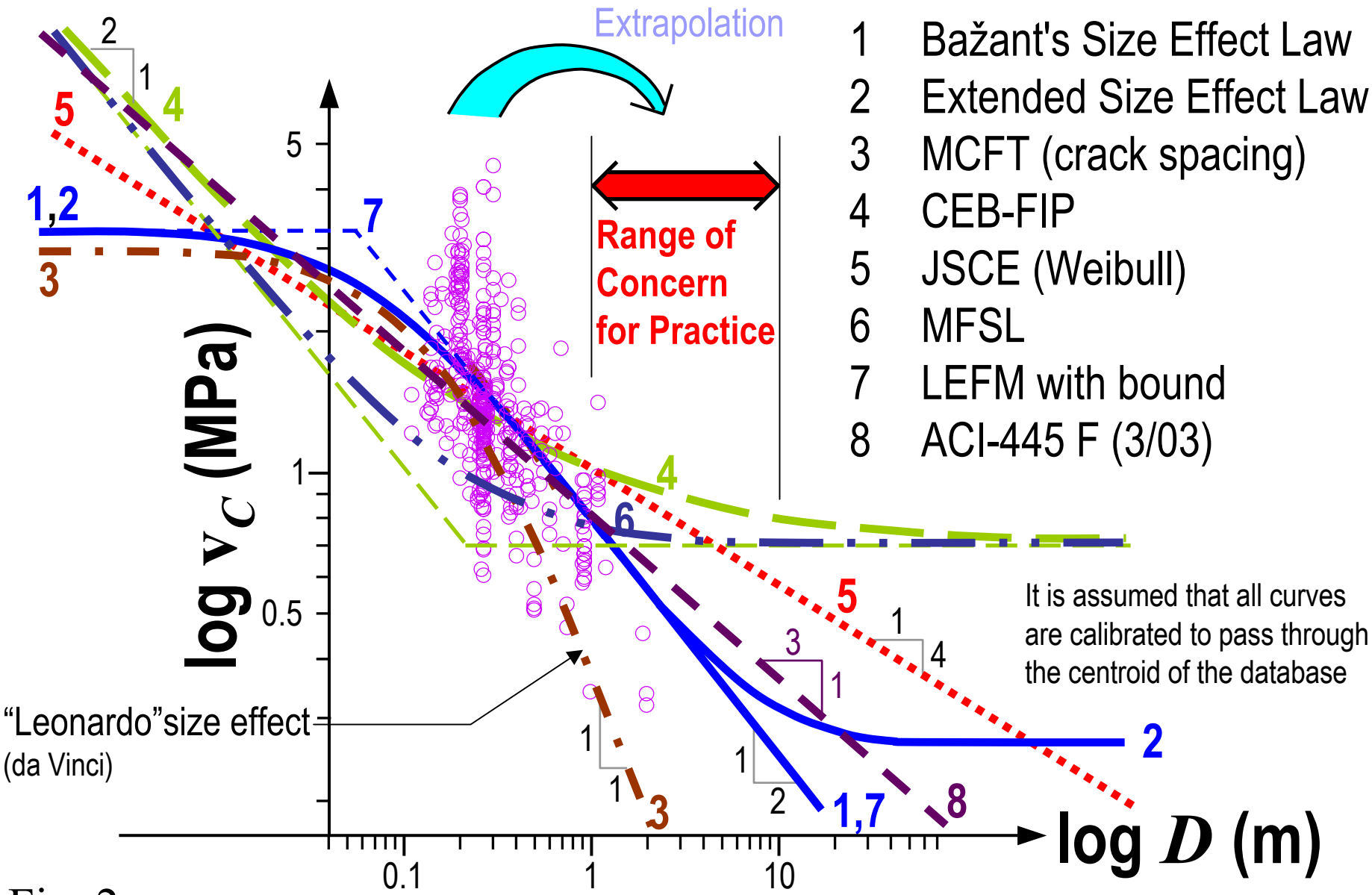
Extrapolation
1 Bažant's Size Effect Law
2 Extended Size Effect Law
3 MCFT (crack spacing)
4 CEB-FIP
5 JSCE (Weibull)
6 MFSL
7 LEFM with bound
8 ACI-445 F (3/03)
Range of Concern for Practice
log $v_C$ (MPa)
log $D$ (m)
5
1
0.5
0.1
1
10
2
1
4
5
1,2
3
7
6
1
4
5
3
1
1
1
3
1
2
1,7
8
2
"Leonardo"size effect
(da Vinci)
It is assumed that all curves are calibrated to pass through the centroid of the database

Fig. 2

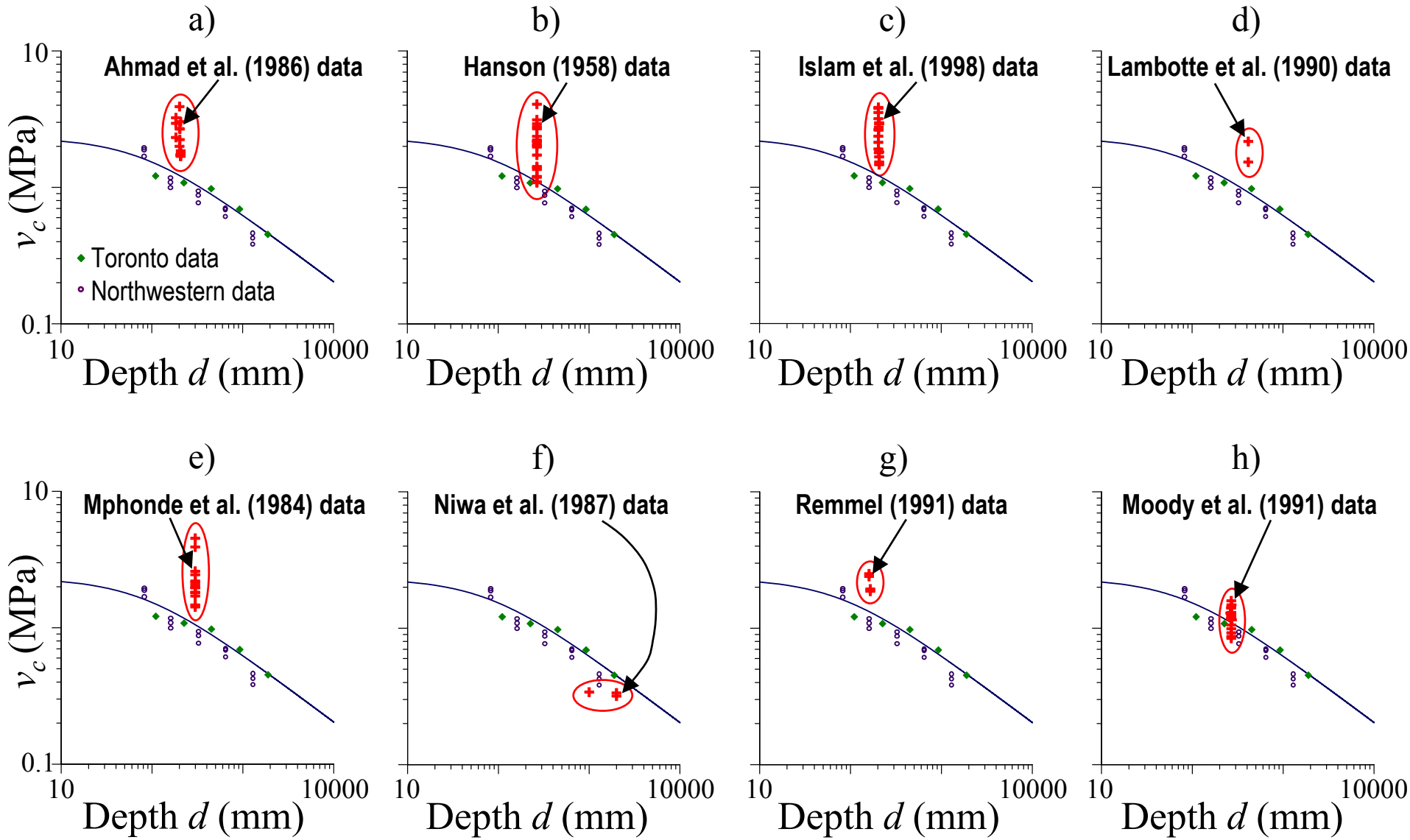
a)
b)
c)
d)
e)
f)
g)
h)
Ahmad et al. (1986) data
Hanson (1958) data
Islam et al. (1998) data
Lambotte et al. (1990) data
Mphonde et al. (1984) data
Niwa et al. (1987) data
Remmel (1991) data
Moody et al. (1991) data
Toronto data
Northwestern data
$v_c$ (MPa)
Depth $d$ (mm)
10
0.1
10000

Fig. 3

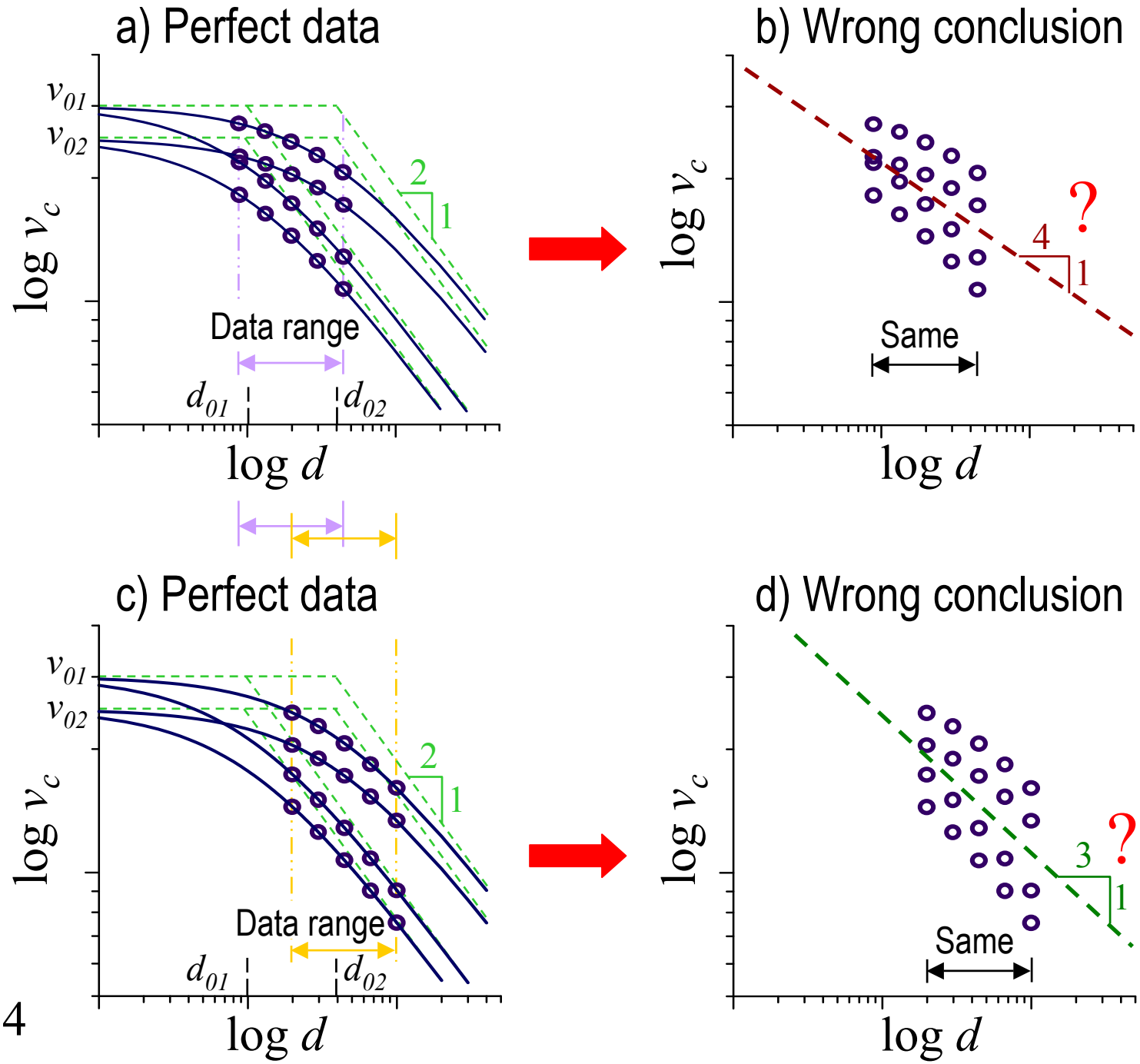
a) Perfect data
$v_{01}$
$v_{02}$
log $v_c$
2
1
Data range
$d_{01}$
$d_{02}$
log $d$
b) Wrong conclusion
log $v_c$
4
1
?
Same
log $d$
c) Perfect data
$v_{01}$
$v_{02}$
log $v_c$
2
1
Data range
$d_{01}$
$d_{02}$
log $d$
d) Wrong conclusion
log $v_c$
3
1
?
Same
log $d$

Fig. 4

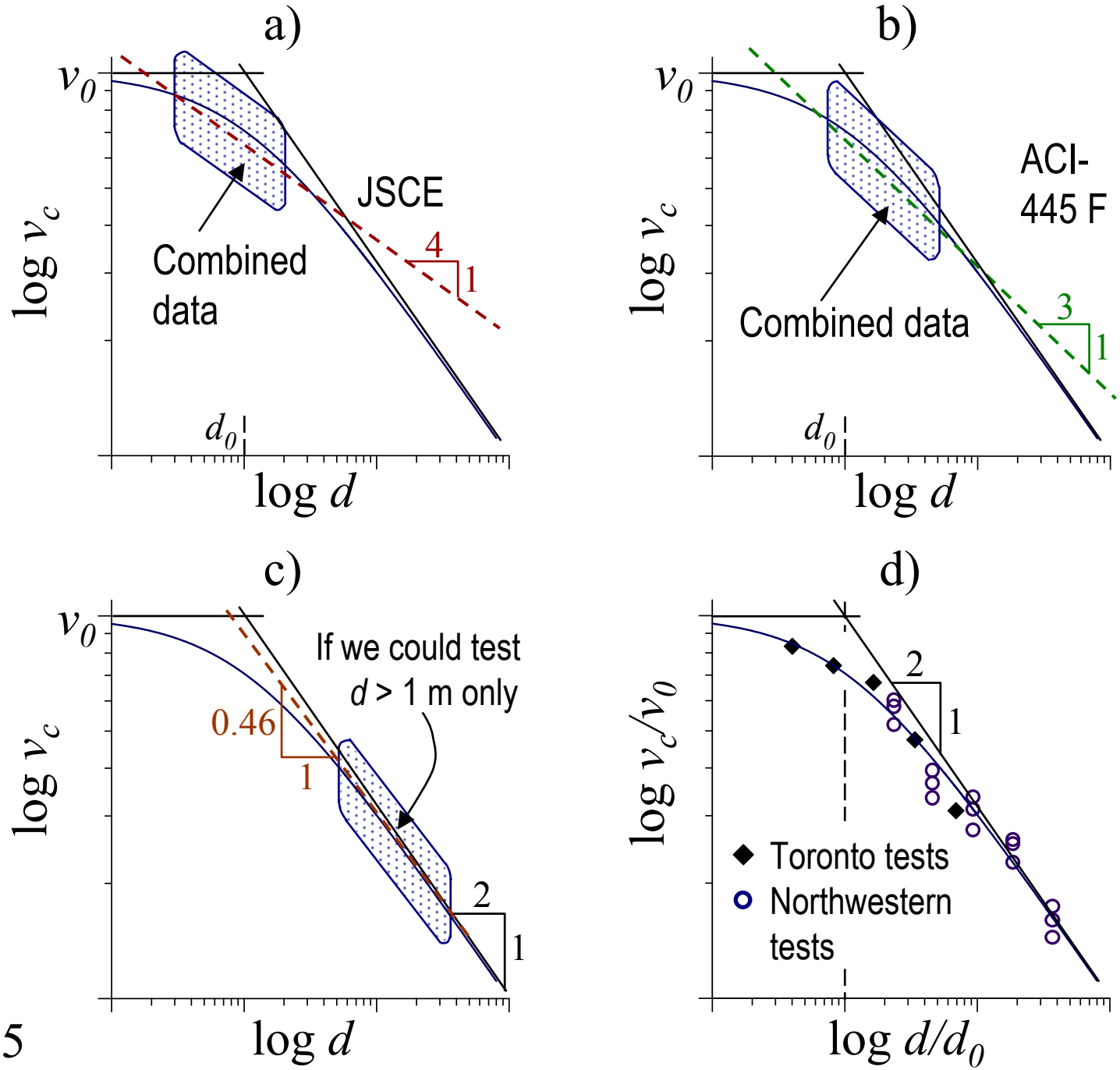
a)
$v_0$
log $v_c$
JSCE
4
1
Combined data
$d_0$
log $d$
b)
$v_0$
log $v_c$
ACI-445 F
3
1
Combined data
$d_0$
log $d$
c)
$v_0$
log $v_c$
If we could test $d$ > 1 m only
0.46
1
2
1
log $d$
d)
log $v_c/v_0$
2
1
Toronto tests
Northwestern tests
log $d/d_0$

Fig. 5

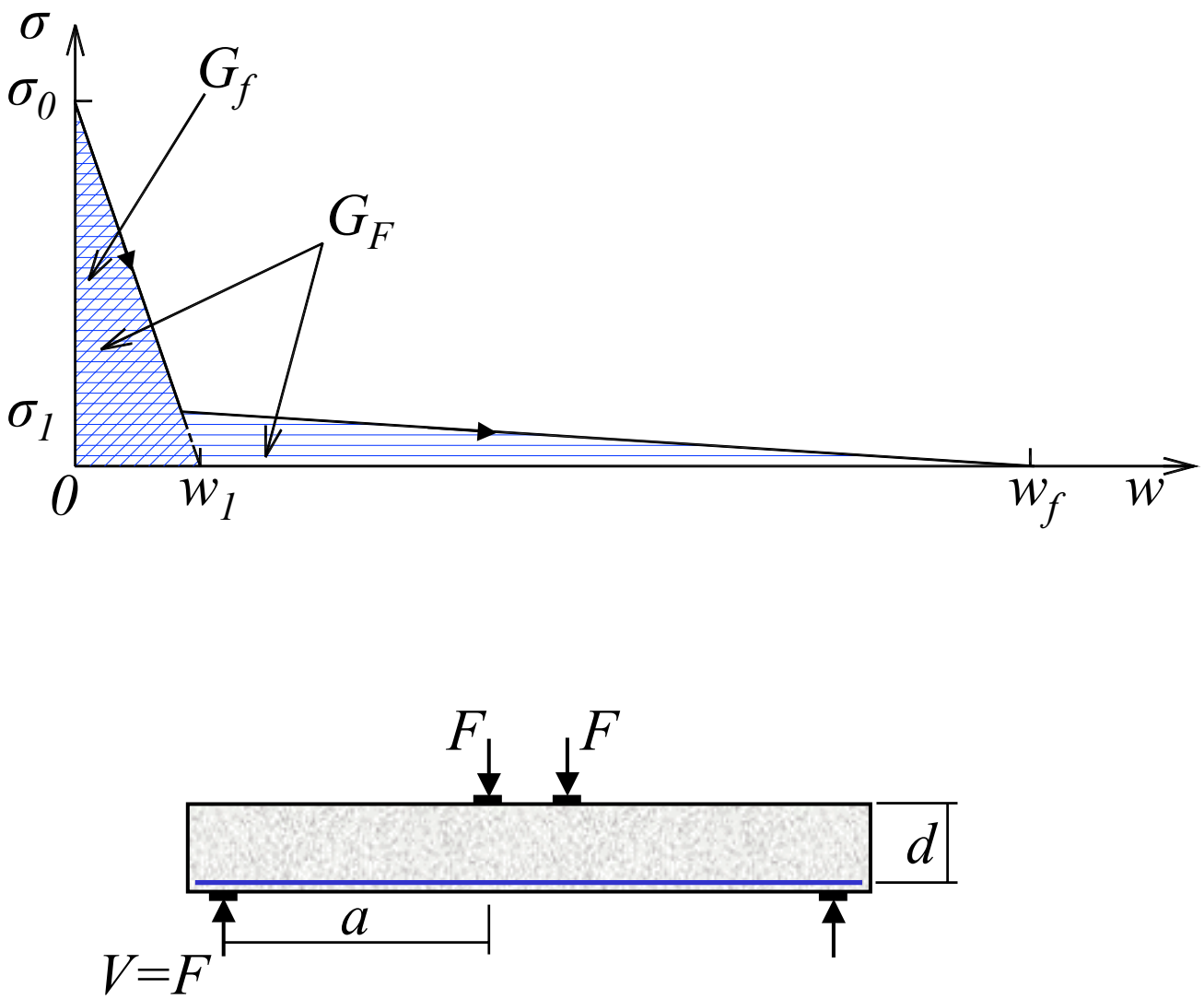


Fig. 6

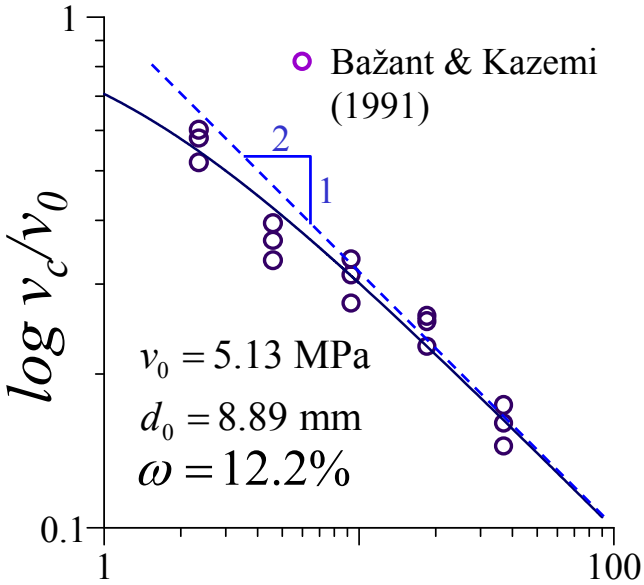
Bažant & Kazemi
(1991)
$v_0 = 5.13$ MPa
$d_0 = 8.89$ mm
$\omega = 12.2\%$
$\log v_c/v_0$
2
1
1
0.1
1
100

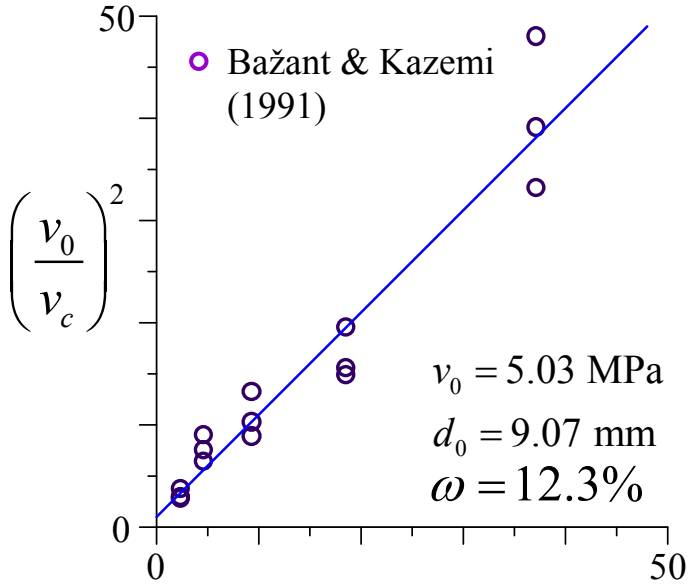
Bažant & Kazemi
(1991)
$v_0 = 5.03$ MPa
$d_0 = 9.07$ mm
$\omega = 12.3\%$
$\left(\frac{v_0}{v_c}\right)^2$
50
0
0
50

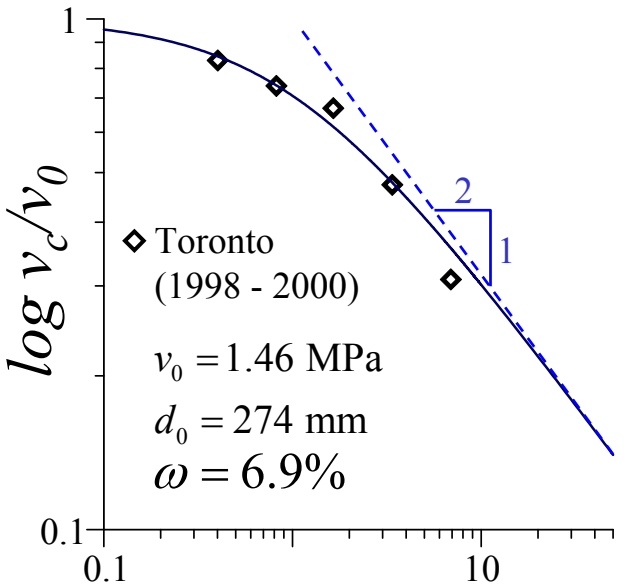
Toronto
(1998 - 2000)
$v_0 = 1.46$ MPa
$d_0 = 274$ mm
$\omega = 6.9\%$
$\log v_c/v_0$
2
1
1
0.1
0.1
10

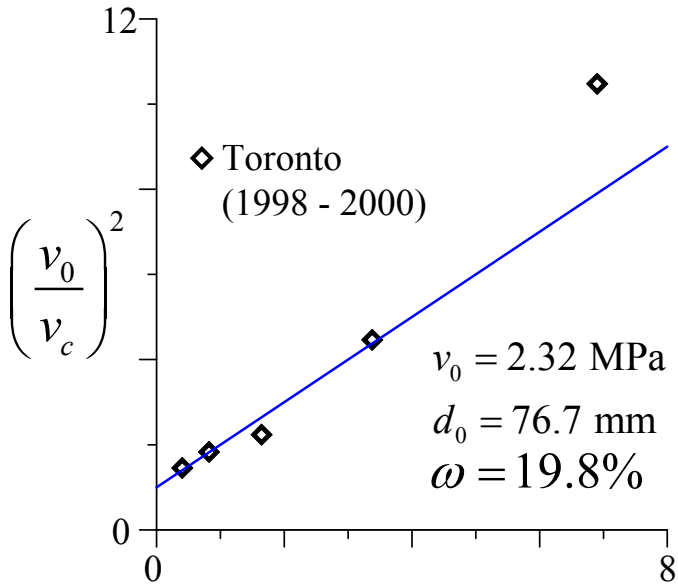
Toronto
(1998 - 2000)
$v_0 = 2.32$ MPa
$d_0 = 76.7$ mm
$\omega = 19.8\%$
$\left(\frac{v_0}{v_c}\right)^2$
12
0
0
8

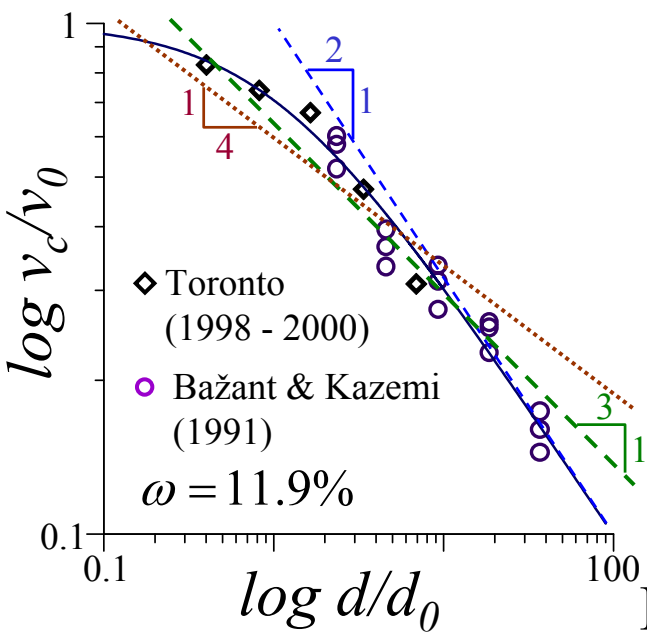
Toronto
(1998 - 2000)
Bažant & Kazemi
(1991)
$\omega = 11.9\%$
$\log v_c/v_0$
2
1
1
4
3
1
1
0.1
0.1
100
$\log d/d_0$

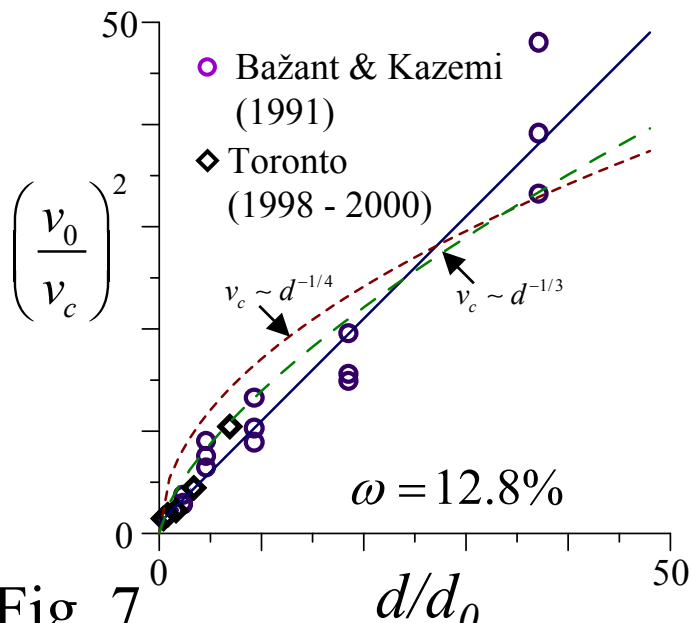
Bažant & Kazemi
(1991)
Toronto
(1998 - 2000)
$v_c \sim d^{-1/4}$
$v_c \sim d^{-1/3}$
$\omega = 12.8\%$
$\left(\frac{v_0}{v_c}\right)^2$
50
0
0
50
$d/d_0$

Fig. 7

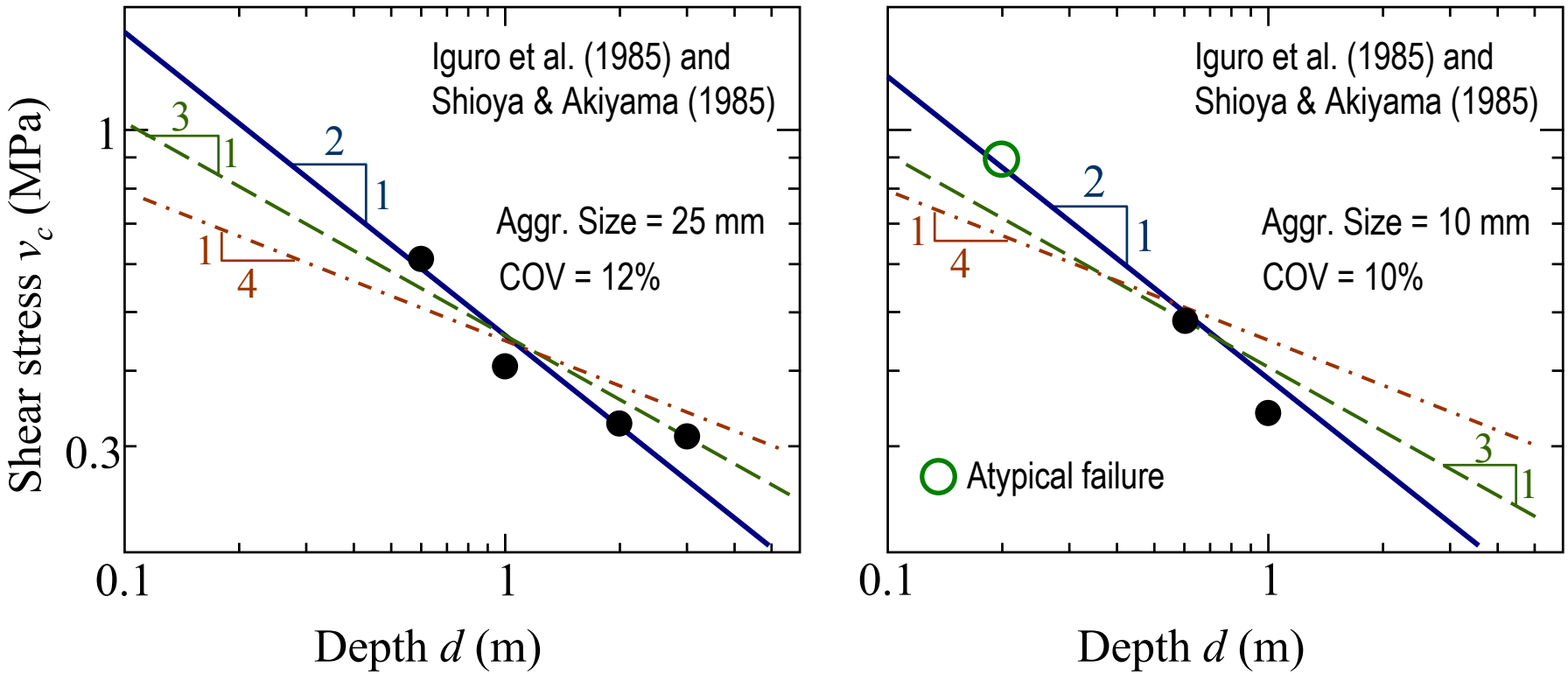
Shear stress $v_c$ (MPa)
1
0.3
0.1
1
Depth $d$ (m)
Iguro et al. (1985) and
Shioya & Akiyama (1985)
Aggr. Size = 25 mm
COV = 12%
3
1
2
1
1
4
Iguro et al. (1985) and
Shioya & Akiyama (1985)
Aggr. Size = 10 mm
COV = 10%
Atypical failure
2
1
1
4
3
1
0.1
1
Depth $d$ (m)

Fig. 8

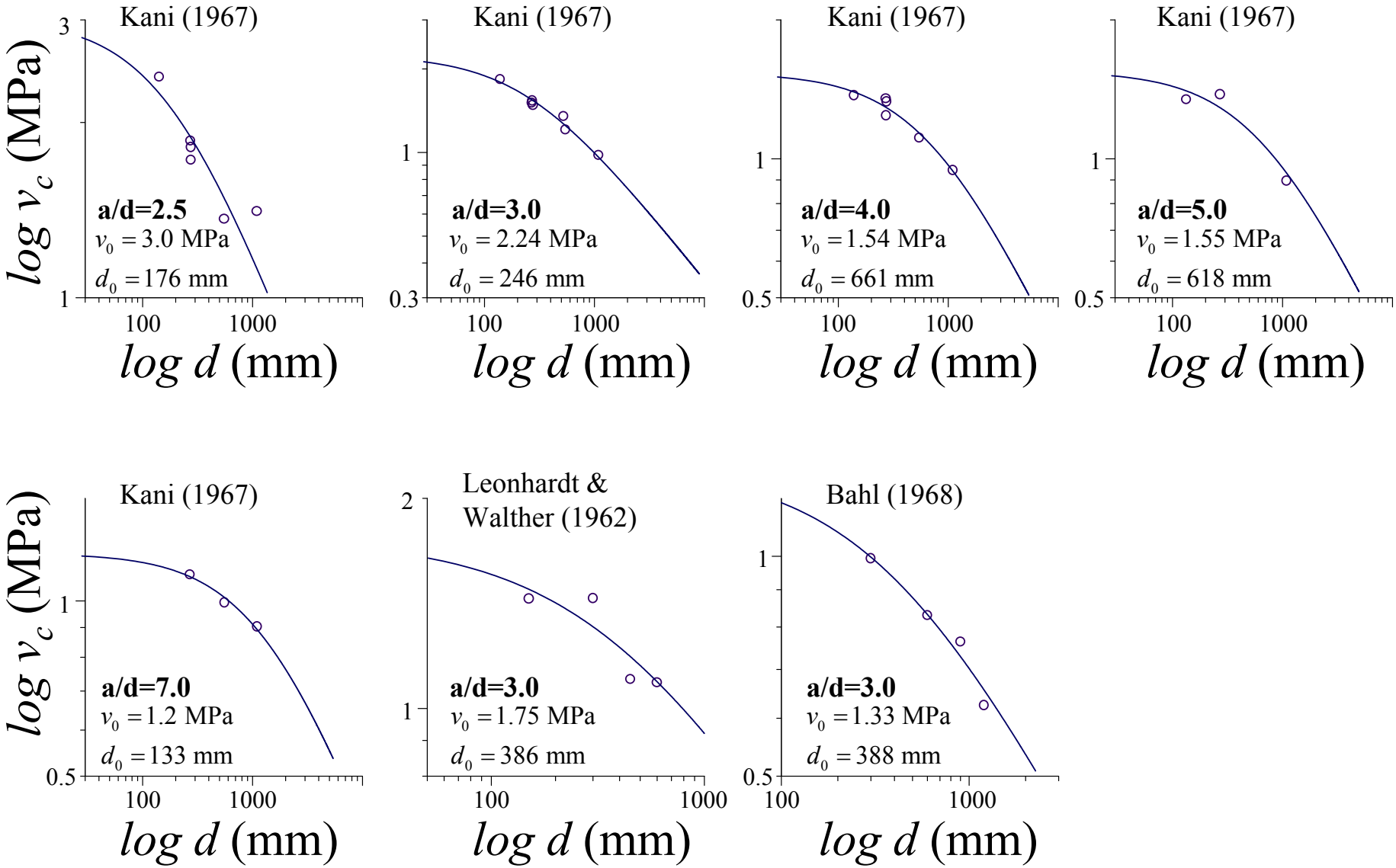
Kani (1967)
a/d=2.5
$v_0$ = 3.0 MPa
$d_0$ = 176 mm
Kani (1967)
a/d=3.0
$v_0$ = 2.24 MPa
$d_0$ = 246 mm
Kani (1967)
a/d=4.0
$v_0$ = 1.54 MPa
$d_0$ = 661 mm
Kani (1967)
a/d=5.0
$v_0$ = 1.55 MPa
$d_0$ = 618 mm
Kani (1967)
a/d=7.0
$v_0$ = 1.2 MPa
$d_0$ = 133 mm
Leonhardt & Walther (1962)
a/d=3.0
$v_0$ = 1.75 MPa
$d_0$ = 386 mm
Bahl (1968)
a/d=3.0
$v_0$ = 1.33 MPa
$d_0$ = 388 mm
log $v_c$ (MPa)
log $d$ (mm)
100
1000

Fig. 9

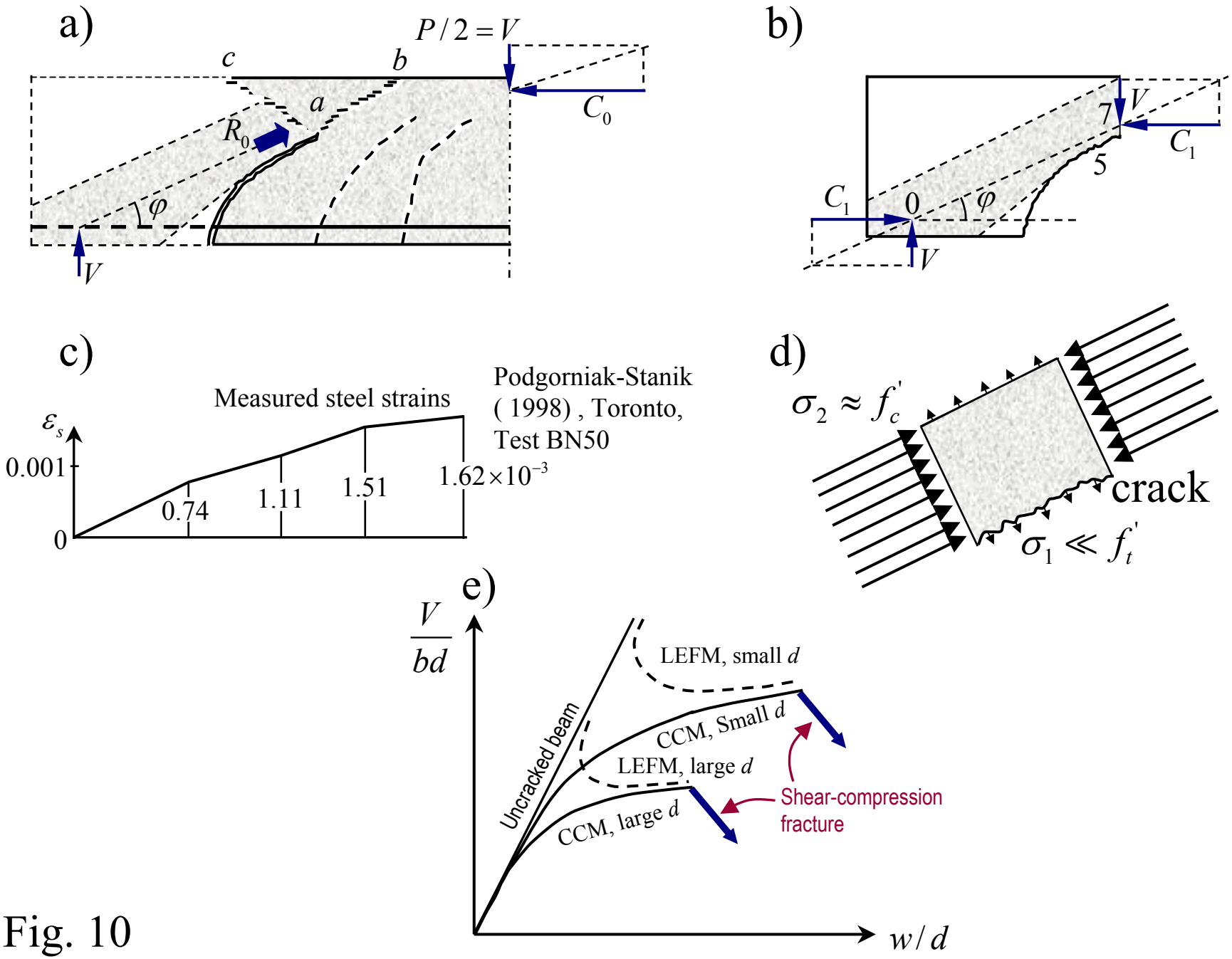
a)
P / 2 = V
c
b
a
C0
R0
φ
V
b)
7
V
C1
5
C1
0
φ
V
c)
Measured steel strains
Podgorniak-Stanik
( 1998) , Toronto,
Test BN50
εs
0.001
0
0.74
1.11
1.51
1.62×10−3
d)
σ2 ≈ f'c
crack
σ1 ≪ f't
e)
V / bd
LEFM, small d
CCM, Small d
LEFM, large d
CCM, large d
Uncracked beam
Shear-compression
fracture
w / d

Fig. 10

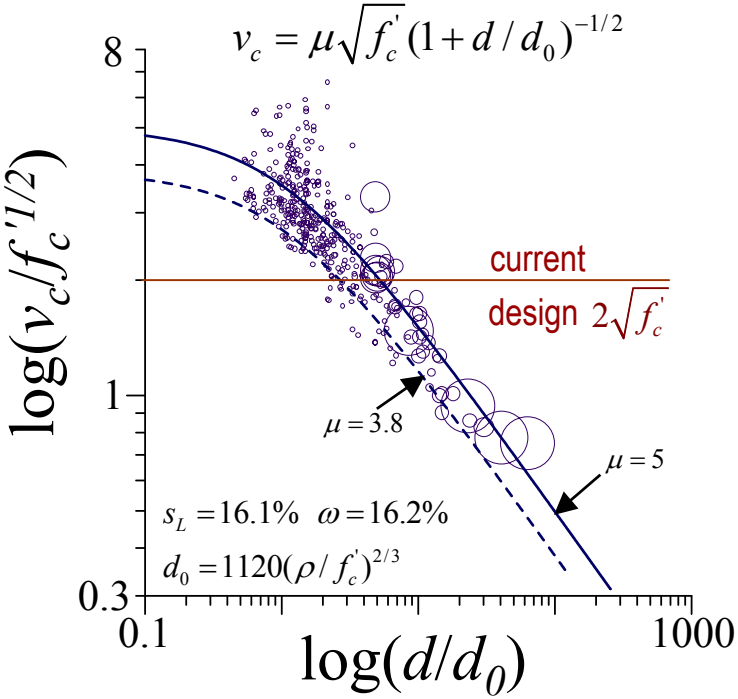
$v_c = \mu\sqrt{f_c'}(1+d/d_0)^{-1/2}$
8
1
0.3
0.1
1000
$\log(v_c/f_c'^{1/2})$
$\log(d/d_0)$
current
design $2\sqrt{f_c'}$
$\mu = 3.8$
$\mu = 5$
$s_L = 16.1\%$ $\omega = 16.2\%$
$d_0 = 1120(\rho/f_c')^{2/3}$

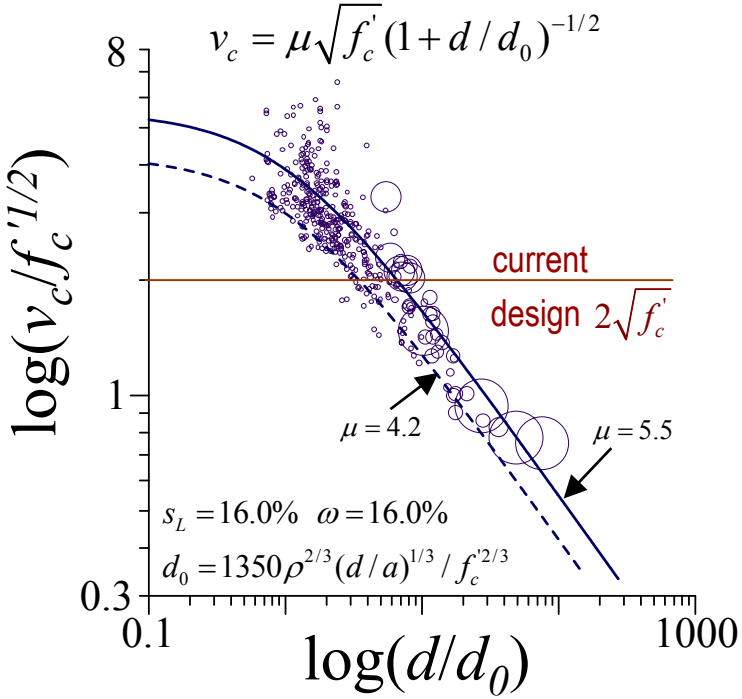
$v_c = \mu\sqrt{f_c'}(1+d/d_0)^{-1/2}$
8
1
0.3
0.1
1000
$\log(v_c/f_c'^{1/2})$
$\log(d/d_0)$
current
design $2\sqrt{f_c'}$
$\mu = 4.2$
$\mu = 5.5$
$s_L = 16.0\%$ $\omega = 16.0\%$
$d_0 = 1350\rho^{2/3}(d/a)^{1/3}/f_c'^{2/3}$

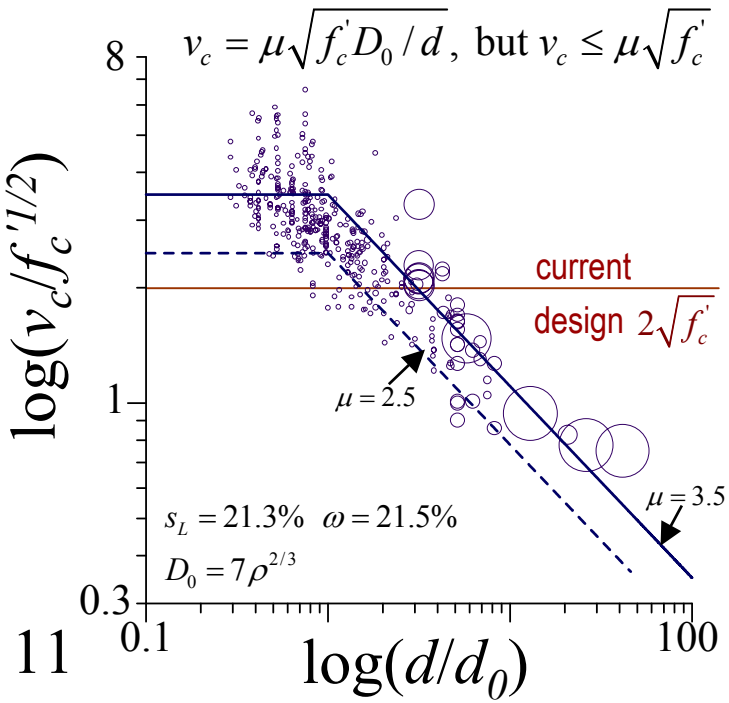
$v_c = \mu\sqrt{f_c' D_0/d}$, but $v_c \le \mu\sqrt{f_c'}$
8
1
0.3
0.1
100
$\log(v_c/f_c'^{1/2})$
$\log(d/d_0)$
current
design $2\sqrt{f_c'}$
$\mu = 2.5$
$\mu = 3.5$
$s_L = 21.3\%$ $\omega = 21.5\%$
$D_0 = 7\rho^{2/3}$

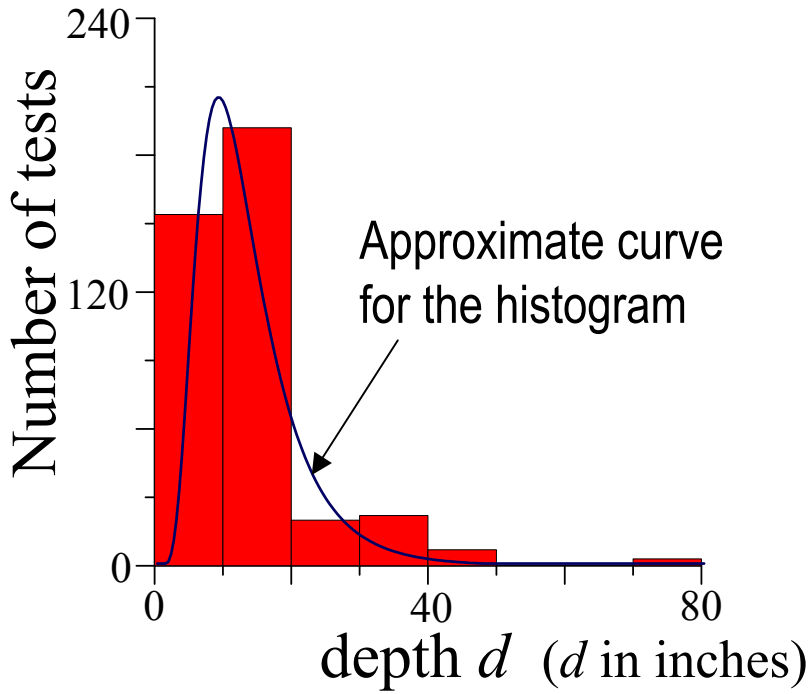
240
120
0
0
40
80
Number of tests
depth $d$ ($d$ in inches)
Approximate curve
for the histogram

Fig. 11

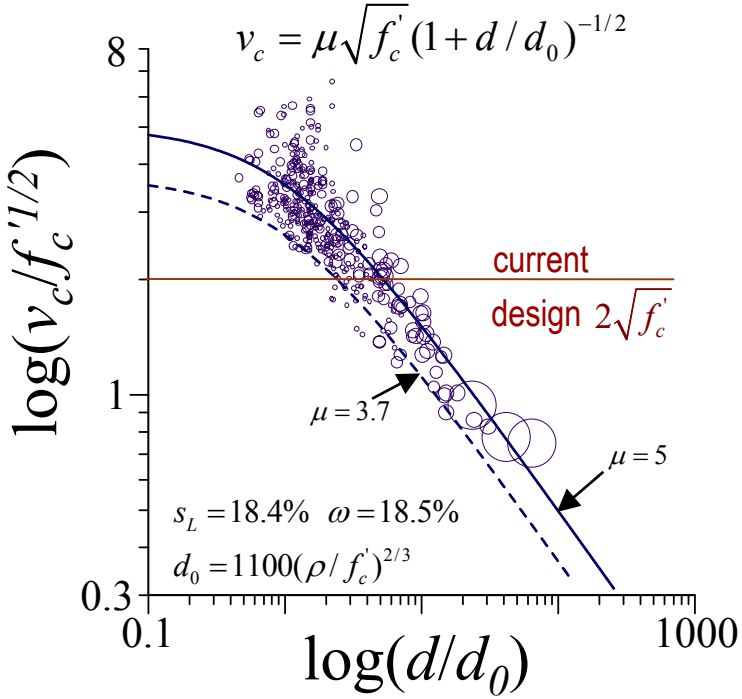
$v_c = \mu\sqrt{f_c'}(1+d/d_0)^{-1/2}$
8
1
0.3
0.1
1000
$\log(v_c/f_c'^{1/2})$
$\log(d/d_0)$
current
design $2\sqrt{f_c'}$
$\mu = 3.7$
$\mu = 5$
$s_L = 18.4\%$ $\omega = 18.5\%$
$d_0 = 1100(\rho/f_c')^{2/3}$

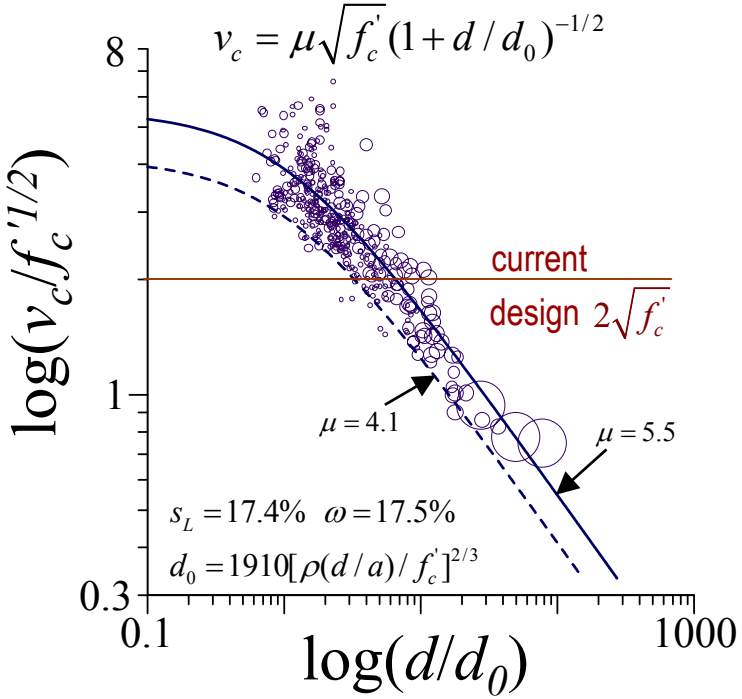
$v_c = \mu\sqrt{f_c'}(1+d/d_0)^{-1/2}$
8
1
0.3
0.1
1000
$\log(v_c/f_c'^{1/2})$
$\log(d/d_0)$
current
design $2\sqrt{f_c'}$
$\mu = 4.1$
$\mu = 5.5$
$s_L = 17.4\%$ $\omega = 17.5\%$
$d_0 = 1910[\rho(d/a)/f_c']^{2/3}$

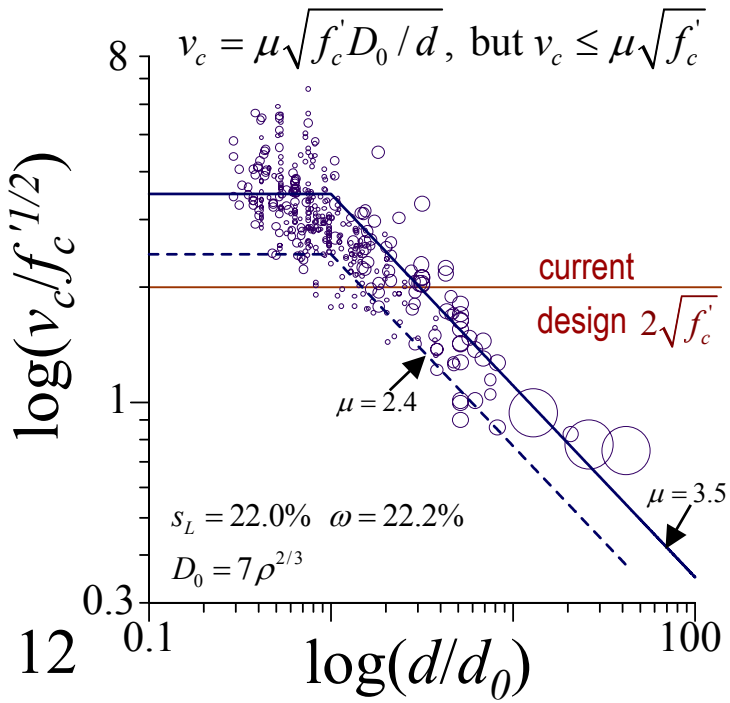
$v_c = \mu\sqrt{f_c' D_0/d}$, but $v_c \le \mu\sqrt{f_c'}$
8
1
0.3
0.1
100
$\log(v_c/f_c'^{1/2})$
$\log(d/d_0)$
current
design $2\sqrt{f_c'}$
$\mu = 2.4$
$\mu = 3.5$
$s_L = 22.0\%$ $\omega = 22.2\%$
$D_0 = 7\rho^{2/3}$

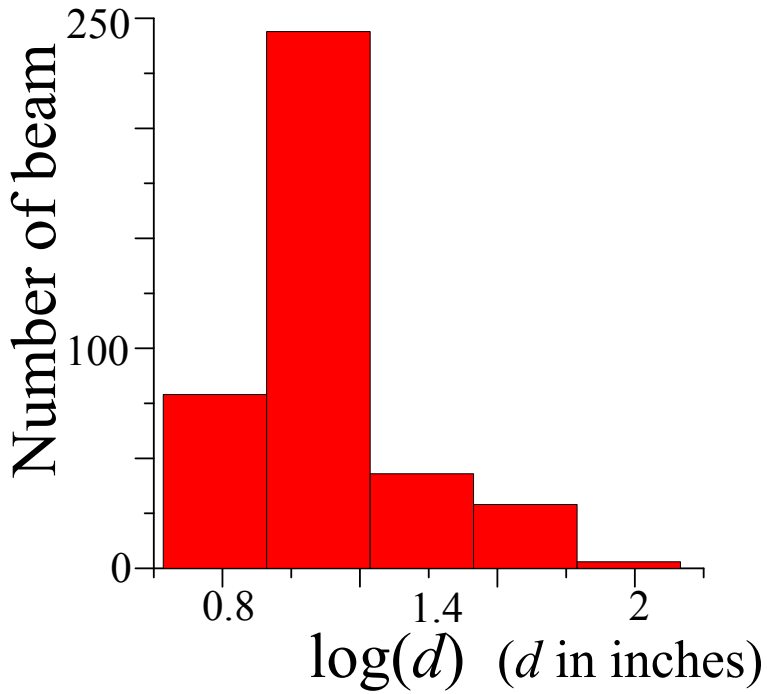
250
100
0
Number of beam
0.8
1.4
2
$\log(d)$ ($d$ in inches)

Fig. 12

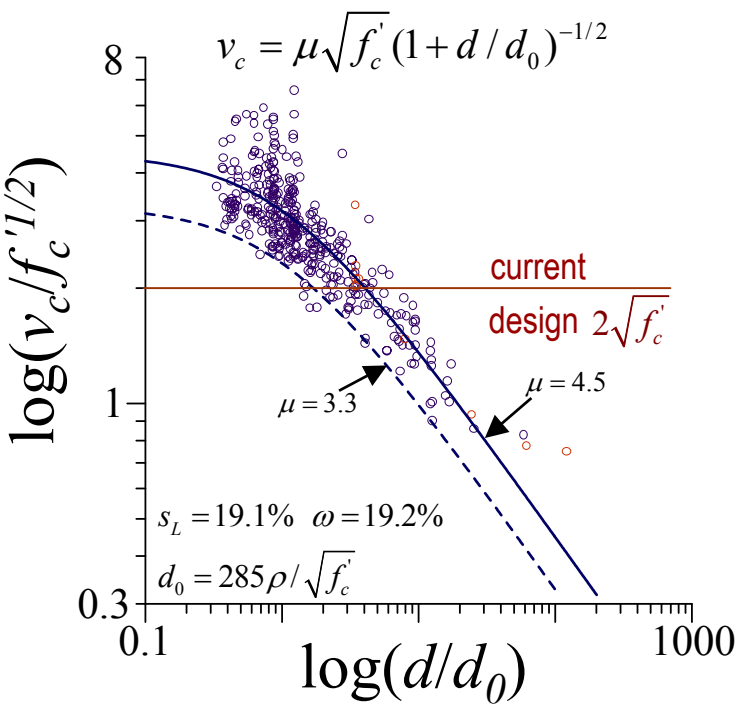
$v_c = \mu\sqrt{f_c'}(1+d/d_0)^{-1/2}$
8
1
0.3
0.1
1000
$\log(v_c/f_c'^{1/2})$
$\log(d/d_0)$
current
design $2\sqrt{f_c'}$
$\mu = 3.3$
$\mu = 4.5$
$s_L = 19.1\%$ $\omega = 19.2\%$
$d_0 = 285\rho/\sqrt{f_c'}$

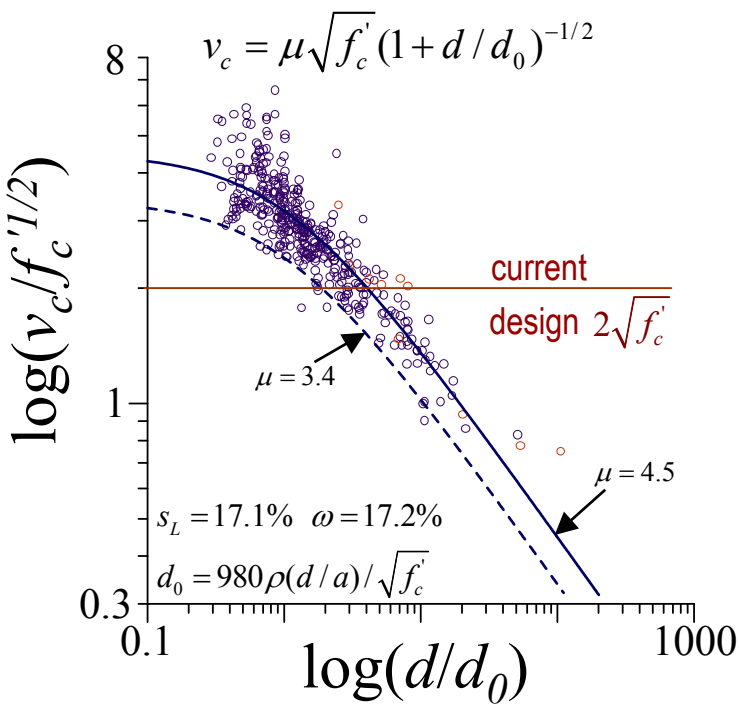
$v_c = \mu\sqrt{f_c'}(1+d/d_0)^{-1/2}$
8
1
0.3
0.1
1000
$\log(v_c/f_c'^{1/2})$
$\log(d/d_0)$
current
design $2\sqrt{f_c'}$
$\mu = 3.4$
$\mu = 4.5$
$s_L = 17.1\%$ $\omega = 17.2\%$
$d_0 = 980\rho(d/a)/\sqrt{f_c'}$

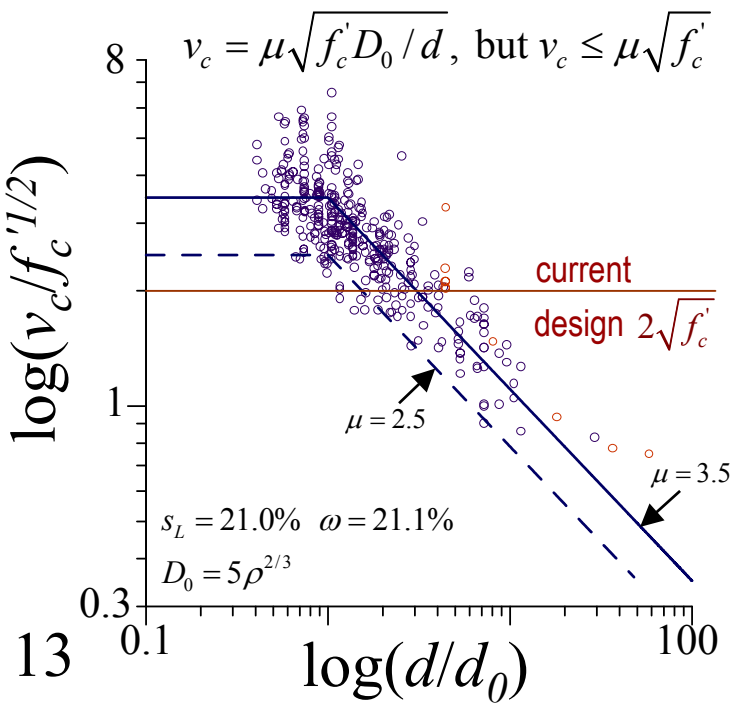
$v_c = \mu\sqrt{f_c' D_0/d}$, but $v_c \le \mu\sqrt{f_c'}$
8
1
0.3
0.1
100
$\log(v_c/f_c'^{1/2})$
$\log(d/d_0)$
current
design $2\sqrt{f_c'}$
$\mu = 2.5$
$\mu = 3.5$
$s_L = 21.0\%$ $\omega = 21.1\%$
$D_0 = 5\rho^{2/3}$

Fig. 13